THE UNIVERSITY OF OKLAHOMA

GRADUATE COLLEGE

SOME EFFECTS PRODUCED BY THE ACTION OF EDDY VISCOSITY ON THE SEMIDIURNAL TIDAL WIND NEAR THE MESOPAUSE

A DISSERTATION

SUBMITTED TO THE GRADUATE FACULTY

in partial fulfillment of the requirements for

the degree of

DOCTOR OF PHILOSOPHY

BY

VICTOR SHELBY WHITEHEAD

Norman, Oklahoma

1968

SOME EFFECTS PRODUCED BY THE ACTION OF EDDY VISCOSITY ON THE SEMIDIURNAL TIDAL WIND NEAR THE MESOPAUSE

APPROVED BY

DISSERTATION COMMITTEE

ACKNOWLEDGEMENTS

The author is indebted to Professor Walter J. Saucier for the opportunity to prepare this paper and the encouragement and counseling he offered during the course of its preparation. He is also indebted to Professors Yoshikazu Sasaki and Eugene M. Wilkins for their technical guidance and encouragement.

Appreciation is also extended to Mary Zimbelman and June Whitehead, who assisted by typing this paper; and to the author's wife, Akemi, whose patience and moral support made its preparation much easier.

A portion of this research was supported by the United States Air Force Cambridge Research Laboratories under Contract 19(628)-4767 to the University of Oklahoma Research Institute.

FOREWORD

This dissertation concerns certain features of that portion of the earth's atmosphere which lies between 85 and 110 kilometers above the earth's surface, that is the upper mesosphere and lower thermosphere. In this region certain natural phenomena occur which are not observed in other atmospheric regions, some of which still lack adequate physical explanation. The work presented in this paper considers only a single aspect of this region, that being the effect large values of eddy viscosity have on the pronounced tidal oscillations observed here. However, it is felt that these effects must be considered in the light of the region's other known and suspected peculiarities, consequently more discussion of environment than usual is given here. No attempt is made to resolve the recently reopened question of the origin of atmospheric tides, although some discussion of this problem is given.

TABLE OF CONTENTS

LIST OF ILLUSTRATIONS

LIST OF SYMBOLS

A_1	amplitude of u component of velocity
A_2	amplitude of v component of velocity
D	displacement of phase of v from u
$F_{\downarrow}$	flux of heat due to eddy mixing
H	scale height
J	heat
K	coefficient of eddy viscosity
K_T	coefficient of eddy thermal diffusivity
L	wavelength
Q	vertical shear of horizontal wind
R	gas constant for dry air
T	period of oscillation
T*	temperature
TFF	tidal forcing function
$\mathbb{V}$	vector wind
b	defines increase of density with height ($\rho = \rho_o e^{bz}$)
c	defines increase of K with height ($K = K_o e^{cz}$)
f	Coriolis parameter
g	acceleration of gravity
p_{ij}	viscous stress
r	radius of earth
t	time
u	wind component from west

v	wind component from south
z	height
Ω	tidal potential
γ	ratio of specific heats
η	molecular kinematic viscosity
θ	latitude
θ^*	potential temperature
μ	coefficient of viscosity
ρ	density
ϕ	longitude
ϕ^*	phase angle of tide
χ	divergence of velocity
ω	angular velocity of earth

SOME EFFECTS PRODUCED BY THE ACTION OF EDDY VISCOSITY ON THE SEMIDIURNAL TIDAL WIND NEAR THE MESOPAUSE

CHAPTER I

INTRODUCTION

The effects of both molecular and eddy viscosity on atmospheric motions are small enough to be considered insignificant in many areas of meteorology. Molecular viscosity has very little effect on atmospheric circulation except very near the surface (less than 1 m) and at altitudes above about 110 km. Elsewhere eddy viscosity is so much greater that it masks the effects of the molecular term. Even the effects of eddy viscosity are generally ignored in many meteorological applications due in part, perhaps, to the uncertainty of their magnitude, but primarily because of their relatively small contribution over the period of interest.

The coefficient of eddy viscosity (K) generally increases with height (decreasing density). In the boundary layer, i.e. from the surface to about 300 m above, K ranges between 1.5×10^4 cm^2/sec and 1.8×10^5 cm^2/sec (Haltiner and Martin, 1957), while in the upper mesosphere values as great as 3×10^6 cm^2/sec are indicated (Johnson and Wilkins, 1965a). This increase in K with height infers an enhanced importance of the viscous terms in the equations of motion for the upper mesosphere and lower thermosphere, a notable characteristic of these

regions. Between 110 and 120 km molecular viscosity becomes equal to the eddy terms (the turbopause) resulting in a suppression of eddy motions and eventual diffusive equilibrium.

The upper mesosphere and lower thermosphere are further characterized by other unique or enhanced phenomena. Of particular interest is the fact that here the tide generated winds exhibit their greatest amplitude, the semidiurnal tide demonstrating a significant phase shift with height (Greenhow and Neufeld, 1955). As a result both zonal and meridional tidal wind profiles contain regions of notable curvature where the effects of viscosity should be significant. In addition to the relatively large semidiurnal wind oscillation, large vertical shears in the horizontal wind component appear here. These shears are much greater than tidal motions would directly support and appear to be the result of a periodic perturbation in height. The most likely explanation of these perturbations has been presented by Hines (1960). He shows that internal gravity waves propagating from denser lower levels, with little decay in their longer wavelengths, will grow in amplitude as the density decreases, until such time that viscous effects become pronounced. Wind observation through the mesosphere, taken by means of rockets, tend to support this theory as they display perturbation throughout, although of small amplitude and quite chaotic in the lower mesosphere. The growth of amplitude with height appears to be that required for an upward propagating waveform, in that kinetic energy per unit mass seems to decrease, but only slightly, with altitude for the longer wavelengths. However, Hines (1963) has also suggested an alternate explanation of the large amplitude oscillation of the upper

mesosphere. Tidal theory indicates (Weekes and Wilkes, 1947) that the ratio of tidal perturbation pressure over ambient pressure increases rapidly between 80 and 100 km, becoming almost 0.2 at 100 km. With such large pressure variations, non-linear effects become important and some sort of cascade of energy into smaller scales of motion may occur.

There exists another physical process which could possibly account for the generation of these perturbations, that being a periodic viscous term acting on the tidal wind field. This process is suggested because of the orderly nature of the perturbation in the vicinity of the mesopause, compared to the noise of the lower levels. Kochanski (1964) has even suggested the perturbation might be some sort of standing wave.

There has been little effort made to determine the effects the large viscous terms have on the tidal motions of the mesosphere and lower thermosphere, even though the determination of these effects could offer much needed insight into the nature of the observed tidal phenomena. This paper attempts to resolve some of the viscous effects. In particular it attempts to determine the difference in phase and amplitude of the tidal forcing function between simple tidal models where K varies from model to model. It also attempts to demonstrate and compare the effects of various assumed hypothetical viscosity distributions on the tidal winds.

CHAPTER II

OBSERVED ENVIRONMENT OF THE UPPER MESOSPHERE AND LOWER THERMOSPHERE

Temperature

Models of atmospheric structure based on observations which assume hydrostatic considerations are available for the region of interest. The temperature profiles as given by U. S. Standard Atmosphere (COESA, 1962) and the supplemental atmospheres (COESA, 1966) for 45N winter and summer are shown in Figure 1. While the region of prime concern in this paper extends only from 85 km to 110 km, processes occuring beyond either of these arbitrarily established boundaries influence the region between. This is very apparent when the heat balance of the region is considered. In all seasons and at all latitudes lower temperatures prevail at 85 to 90 km (the mesopause) than occur above and below. The principal heat input processes at this level of lower temperatures are:

1) direct absorption of solar radiant energy (about 4/5 of which goes into dissociation of O_2 (Johnson and Wilkins (1965a),
2) molecular conduction from both higher and lower levels,
3) heat released by recombination of 0 by three body collisions,
4) viscous dissipation of kinetic energy, and
5) infrared heating from higher and lower levels

For equilibrium these heat inputs must be balanced by losses. The principal processes involved are:

1) Infrared emission (about 15% of absorbed solar energy), and

2) flux of heat downward due to eddy motions in the presence of increase of potential temperature with height.

Johnson and Wilkins (1965a and b) estimated the maximum coefficient of eddy conductivity and viscosity by considering this balance (excluding viscous heating). They estimated the maximum mean coefficient of eddy viscosity to range from about 300 m^2/sec at 85 km to about 800 m^2/sec at 100 km. This is an increase of a factor of 10 to 100 over the magnitude of this coefficient near the surface.

The effect of the eddy flux term on the temperature structure of the upper mesosphere and lower thermosphere is pronounced. As Figure 1 demonstrates, during the summer when heat input is enhanced, the mesopause is colder than in the winter when this input is reduced. This effect is analogous to that occuring in the lower atmosphere where the summer tropopause is characterized by cooler temperatures than the winter tropopause. In the case of the lower atmosphere, mixing is enhanced by heating of the earth's surface, while through the mesosphere mixing is enhanced by heating of the stratopause (mesospeak) by absorption of solar ultraviolet radiation by ozone. This enhanced mixing (i.e., increase in coefficient of eddy viscosity) during warmer months may have some bearing on seasonal changes in features of the semidiurnal tide observed in the lower thermosphere. Latitudinal departures from standard in temperature are similar to the seasonal changes in that the greater the exposure to sunlight, the colder the upper mesosphere and

lower thermosphere (COESA, 1966).

Besides the seasonal and latitudinal variations, there exist day to day changes associated with synoptic scale and planetary wave disturbances. These changes are masked to a great degree, however, by significant short term variations which appear to be periodic in height. These latter variations are most likely caused by the vertical motions associated with internal gravity waves and tides.

Detailed analysis of the temperature distribution in the upper mesosphere and lower thermosphere is complicated by the fact that temperature is generally a deduced parameter. Direct observations are made difficult due to the problem of ventilation of the sensor.

Winds

Wind observations are probably the most accurate of all observations taken in the upper mesosphere and lower thermosphere. The observations are usually made by ground tracking of a vaporous tracer or falling object. Placing the vapor or object has required the use of rockets, consequently only a small number of observations are available. Recently however, gun launched projectiles have been used at considerable savings (Murphy et al.1966). Another inexpensive observational method particularly effective over the height range of interest is radio observations of meteor trails (Greenhow, 1954). The observations taken at Jodrell Bank Observatory (England) and at Adelaide (Australia) represent the greatest source of wind data for the region of interest and have contributed greatly to the knowledge of processes in this region. Figure 2 is a meridional cross-section of the zonal wind component for January and July (Gringorten et al.1965). This figure represents the

climatology of the zonal wind field, in that significant departures can occur from these mean wind values. The seasonal change in the mesospheric wind field differs from tropospheric seasonal changes in timing and in length of seasons. Long periods of easterly or westerly flow are separated by shorter periods (spring, fall), in which the wind field undergoes relative rapid change. The change appears to propagate downward (Appleman, 1963). The spring transition occurs between 15 March and 31 May, and the fall transition between 15 August and 30 September. Overall there is little seasonal change in meridional flow until above 80 km, where equatorward winds of 10-20 knots are found in summer and poleward winds of 5 knots or so in winter. These meridional winds may be explained as ageostrophic motions resulting in part from viscous effects and are in general agreement with other features of atmospheric structure.

Pronounced diurnal and semidiurnal oscillations occur above 80 km. The semidiurnal oscillation appears to be a major contributor to wind variability in the upper mesosphere and lower thermosphere. These variations appear to be brought about by thermally driven tides. Their amplitudes vary seasonally. At 80 to 100 km the amplitude of the diurnal oscillation is largest in summer and smallest in winter. The reverse is true for the semidiurnal oscillation (Gringorten et al. 1965). These variations in amplitude lack adequate physical explanation. Hines (1963) has suggested such phenomena may be the result of selective filtering by the underlying atmosphere structure.

The semidiurnal oscillation of the winds on a September day, as determined from meteor echos by Greenhow and Neufeld (1956), are shown in Figure 3. Apparent is an increase of amplitude with height along with

a phase shift indicating a downward propagation of the wave forms. The east-west and north-south wind components are roughly 90 degrees out of phase as they should be for essentially circular motion of the air elements. Greenhow and Neufeld (1961) in considering the phase changes that occur in this semidiurnal oscillation with season have found that, at Jodrell Bank, in the early part of the year, maximum velocity towards the north occurs at about 0700 local time. The phase slowly changes at about 10 degrees per month until August when maximum northward velocity occurs at 0400 hours (Figure 3). The rate of change of phase then rapidly increases with the maximum advancing to 0000 hours at 92 km by the first of October, followed by a return to the winter regime. Further, Greenhow and Neufeld found considerable differences in this phase change with season from year to year, suggesting strong dependence of this phenomena on atmospheric structure. There is no obvious factor in tidal theory to explain this variation (Craig, 1965).

Greenhow and Neufeld also found a persisting change in both the phase and amplitude of the semidiurnal component between 85 and 100 km. On the average, the amplitude of the oscillation is larger at 100 km than at 85 km by about 15 m/sec. The mean gradient of phase with height ranges from +7 deg/km in winter to about +3 deg/km in summer. There appears to be no increase in amplitude above 100 km, but the phase gradient appears to continue.

The diurnal wind oscillation does not display this change of phase over this altitude range. Hines (1963) suggests this might imply a local input of diurnal tidal energy. The diurnal tide is considered to be purely thermally driven, so such a local input could be easily

visualized.

At altitudes above about 105 km, systematic observations of the wind requires that a trace be dispersed through the particular altitude of interest. Ionospheric drift measurements are available, but there is no certainty that these observations represent winds. Observations which are available (Manring et al.1964, Rosenberg and Edwards, 1964) show a systematic upward spiral of the wind vector, with rotation normally clockwise with increasing height, in the northern hemisphere, to at least 130-140 km, where the sense of rotation may change (Koshanski, 1964). This continued rotation of the wind vector with height above the level of meteor echo observations is likely an extension of the semidiurnal tidal wind, although there is not yet sufficient data to rule out the diurnal tide as a causitive factor (Hines, 1966).

In addition to the perturbation of the wind due to the tides, observations indicate higher frequency (shorter vertical wavelength) oscillations of almost the same amplitude as the semidiurnal tidal winds, in some instances even greater. To resolve the tidal components these higher frequencies must be filtered (usually by averaging processes). While there is still some question as to their origin (Hines, 1963), the observed phenomena describe conditions which would be expected due to the presence of internal gravity waves. However, Kochanski (1964) has found an orderliness in phase of these smaller perturbations at the altitude where their amplitude is greatest (about 100 km). This orderliness would be unlikely if randomly generated internal gravity waves were their only source. Hines (1963) has suggested an alternate cause of these higher frequency oscillations, that being the cascade of tidal

energy into smaller scale disturbances. There is some indication that internal gravity waves are present at levels above the region of interest. If these are propagated from below, however, the shorter wavelengths should be severely filtered out by viscous action. Hines (1965) has calculated heating rates due to dissipation of internal gravity waves by viscosity to range between 10 K/day at 95 km to 100 K/day at 140 km. He estimates that the heating source competes with solar heating as a primary source of heating in the E region ($\sim$120 km) and suggests that tidal inputs to viscous heating may be comparable. Theoretical evidence that internal gravity waves propagate into the middle thermosphere has been presented by Friedman (1966). By considering a thermally stratified atmosphere, he was able to find propagation modes of internal gravity waves which have properties which are in general agreement with traveling ionospheric disturbances in the F region (>140 km). Georges (1967), using doppler frequency shift techniques at 2.1, 3.3, and 4.0 Mc/s, has found observational evidence of the existence of gravity waves in the thermosphere. He found occasional trains of nearly sinusoidal frequency variation with height lasting for as long as several hours. The observed periods range from tens of seconds to over an hour with those in the 2-5 minute range most common. Periods between 5 and 15 minutes dominated near midday, with periods longer than 15 minutes appearing at night. The daytime periods represent heights just above 100 km, nighttime near 250 km. It appears then that characteristics of internal gravity waves are found both above and below the altitude range studied here, and that there is no physical reason for their nonoccurance between 85 and 110 km. Thus, even if other processes

contribute to the observed large variability of the wind between 85 and 110 km, they likely occur in conjunction with the internal gravity waves.

Tides

Tidal theory is discussed in greater detail in Chapter III along with the presentation of the development of the tidal equation including the viscous term. The discussion in this sub-section is purely descriptive.

The term "atmospheric tide" is used to refer to atmospheric oscillations whose periods are equal to or sub-multiples of the lunar or solar day. These oscillations may be either gravitationally or thermally driven or some combination of both. The atmospheric tide near the earth's surface reveals oscillations with periods of 12 and 24 hours of about the same amplitude. Much weaker higher harmonics of these modes are found along with a barely detectable component with a period of 12 lunar hours.

The twelve lunar hour tide stems from a purely gravitational source, while the solar diurnal tide is essentially thermally driven. The observed tidal distribution poses two questions. First, why is the lunar tide so small compared to the semidiurnal solar tide? Secondly, why is the semidiurnal solar tide equal in magnitude to the diurnal component when the 24 hour thermal component is so much greater? Thompson (1882) resolved these discrepancies by assuming the atmosphere has a natural frequency, with a period very near 12 hours, so that successive oscillations of this period are amplified until an equilibrium is reached with the dissipative forces. The driving force for the semidiurnal tide could then be either thermal or gravitational or a combination of both.

Chapman (1924), by considering the phase of the observed semidiurnal oscillations, concluded the thermal contribution is at least equal to the gravitational contribution. Following Thompson, other investigators have made extensive use of the assumption of atmospheric resonance. Among them are Pekeris (1937), Weeks and Wilkes (1947), and Siebert (1961). The development of the tidal equation with viscosity, given in Chapter III follows the treatment by Siebert in which viscosity is neglected.

Recently the question of the necessity for resonance has been reopened by Small and Butler (1961), who concluded that the heating of the ozone layer is adequate to drive the semidiurnal tide, and instead of the semidiurnal tide being amplified the diurnal tide is suppressed. The question of source and to some extent cause of the pronounced semidiurnal, two-wave tide remains open. The great difficulty apparently stems from the fact that the atmosphere is a constantly changing medium most difficult to duplicate by modeling.

Most of the characteristics of tides in the region of interest, as indicated by tidal winds, were discussed previously under Winds, and will not be repeated here. Because both pressure and temperature are difficult to observe accurately above 70 km, much of the suspected feature of the tidal behavior between 85 and 110 km is based on wind (pp. 7-13) observations and theoretical considerations. The complexities of tidal theory render it inadequate to totally predict the tides which exist, although given tidal observations, models which are capable of duplicating the observations can be constructed. It is common practice to infer tidal pressure wave distribution from the tidal wind data.

This may be misleading in the 85 to 110 km region due to the effects of eddy viscosity on the phase of the wave form. This factor has not been considered in the past.

It should be noted that the questions concerning the tides in the lower atmosphere persist in the region of interest and are in fact further complicated by additional uncertainties. For example, it has generally been accepted in the past that the semidiurnal tide here was of the same mode (two wave-lengths around the globe) as found at the surface. Hines (1966) however, has suggested that instead, the observed tidal winds may be the result of the first harmonic of the two-wave tide. Whatever its source, the semidiurnal tide becomes increasingly important, compared to the diurnal tide, between 85 and 110 km. Roper (1966) has shown that over the altitude range 83 to 97 km, the ratio of energy of semidiurnal to diurnal tide increased from about 1/5 to 5/3.

CHAPTER III

DEVELOPMENT OF TIDAL EQUATION WITH VISCOSITY

The development of the tidal equation presented here is essentially that given by Siebert (1961), except that the viscous term is included in the equation of horizontal motion. Two minor changes are also made. Latitude is used rather than co-latitude and the components of motion are defined so that u represents a wind from the west, v, a wind from the south. These minor changes are made to follow common meteorological nomenclature used elsewhere in this paper.

The set of basic equations consists of the two linearized equations of horizontal motion:

$$\frac{\partial u}{\partial t} = 2\omega\, v \sin\theta - \frac{1}{r\cos\theta}\,\frac{\partial}{\partial\varphi}\left(\frac{\delta P}{\rho_o} + \Omega\right) + \frac{1}{\rho_o}\,\frac{\partial}{\partial z}\left(\rho_o K \frac{\partial u}{\partial z}\right) \qquad (3.1)$$

$$\frac{\partial v}{\partial t} = -2\omega\, u \sin\theta - \frac{1}{r}\,\frac{\partial}{\partial\theta}\left(\frac{\delta P}{\rho_o} + \Omega\right) + \frac{1}{\rho_o}\,\frac{\partial}{\partial z}\left(\rho_o K \frac{\partial v}{\partial z}\right), \qquad (3.2)$$

the hydrostatic equation

$$\frac{\partial \delta P}{\partial z} = -g\,\delta\rho - \rho_o\,\frac{\partial\Omega}{\partial z}, \qquad (3.3)$$

the equation of continuity

$$\frac{D\rho}{Dt} + \rho_o \chi = 0 \qquad (3.4)$$

or,

$$\frac{\partial \delta\rho}{\partial t} = -w\,\frac{\partial \rho_o}{\partial z} - \rho_o\chi, \qquad (3.5)$$

where

$$\text{Div}\,\mathbf{V} = \chi = \frac{1}{r\cos\theta}\frac{\partial}{\partial\theta}(v\cos\theta) + \frac{1}{r\cos\theta}\frac{\partial u}{\partial\varphi} + \frac{\partial\omega}{\partial z} \tag{3.6}$$

and, the thermodynamic equation

$$\frac{\partial\delta P}{\partial t} = \gamma gH(-\rho_o\chi) + (\gamma-1)\rho_o J + w\rho_o g, \tag{3.7}$$

where the differential operator

$$\frac{D\rho}{Dt} = w\frac{d\rho_o}{dz} + \frac{\partial\delta\rho}{\partial t}$$

and

r is radius of earth,

θ is latitude,

φ is longitude,

γ is the ratio of specific heats,

H is scale height of atmosphere, and

J is heat input.

By taking the derivative of (3.3) with time

$$\frac{\partial}{\partial z}\left(\frac{\partial\delta P}{\partial t}\right) = -g\frac{\partial\delta\rho}{\partial t} - \rho_o\frac{\partial}{\partial t}\left(\frac{\partial\Omega}{\partial z}\right) \tag{3.8}$$

and substituting for $\partial\delta\rho/\partial t$ from (3.4)

$$\frac{\partial}{\partial z}\left(\frac{\partial\delta P}{\partial t}\right) = gw\frac{\partial\rho_o}{\partial z} + g\rho_o\chi - \rho_o\frac{\partial}{\partial t}\frac{\partial\Omega}{\partial z} \tag{3.9}$$

$\delta\rho$ is eliminated.

The variables u, v, w, δP, $\delta\rho$, δT, χ, and J are periodic in time and over at least a major part of one wavelength appear periodic with height, so let u, v, w, $\delta\rho$, δT, χ, and J be proportional to $e^{i(\sigma t + nz)}$. Substitution of the above definitions into (3.1) and (3.2) results in

$$u = \frac{2\omega v \sin\theta - \frac{1}{r\cos\theta}\frac{\partial}{\partial\theta}\left(\frac{\delta P}{\rho_o} + \Omega\right)}{\left\{i\sigma + n^2K - in\frac{\partial K}{\partial z} - inK\left(\frac{1}{\rho_o}\frac{\partial \rho_o}{\partial z}\right)\right\}} \tag{3.10}$$

and

$$v = \frac{-2\omega u \sin\theta - \frac{1}{r}\frac{\partial}{\partial\theta}\left(\frac{\delta P}{\rho_o} + \Omega\right)}{\left\{i\sigma + n^2K - in\frac{\partial K}{\partial z} - inK\left(\frac{1}{\rho}\frac{\partial \rho_o}{\partial z}\right)\right\}} . \tag{3.11}$$

If the term in $\left\{\ \right\}$ is denoted by S and $2\omega\sin\varphi$ by f, then (3.11) becomes

$$vS = -fu - \frac{1}{r}\frac{\partial}{\partial\theta}\left(\frac{\delta P}{\rho_o} + \Omega\right). \tag{3.12}$$

Substituting (3.10) into (3.12) and solving for v results in

$$v = \left[\frac{\frac{f}{r\cos\theta}\frac{\partial}{\partial\varphi} - \frac{S}{r}\frac{\partial}{\partial\theta}}{S^2 + f^2}\right]\left(\frac{\delta P}{\rho_o} + \Omega\right), \tag{3.13}$$

Similarly,

$$u = \left[\frac{\frac{-f}{r}\frac{\partial}{\partial\theta} - \frac{S}{r\cos\theta}\frac{\partial}{\partial\varphi}}{S^2 + f^2}\right]\left(\frac{\delta P}{\rho_o} + \Omega\right), \tag{3.14}$$

Substitution of (3.6) and (3.13) into (3.14) yields

$$\chi - \frac{\partial w}{\partial z} = \left\{\frac{1}{r\cos\theta}\frac{\partial}{\partial\theta}\left[\frac{(\cos\theta)\left(\frac{f}{r\cos\theta}\frac{\partial}{\partial\varphi} - \frac{S}{r}\frac{\partial}{\partial\theta}\right)}{S^2 + f^2}\right] + \frac{1}{r\cos\theta}\frac{\partial}{\partial\varphi}\left[\frac{\left(-\frac{f}{r}\frac{\partial}{\partial\theta} - \frac{S}{r\cos\theta}\frac{\partial}{\partial\varphi}\right)}{S^2 + f^2}\right]\right\}\left(\frac{\delta P}{\rho_o} + \Omega\right)$$

or

$$\chi - \frac{\partial w}{\partial z} = F\left(\frac{\delta P}{\rho_o} + \Omega\right) \tag{3.15}$$

where F is the operator in $\left\{\ \right\}$.

Now differentiation of (3.7) with height and equating the resulting expression to (3.9) yields

$$\rho_o g \frac{\partial w}{\partial z} = \gamma g \frac{\partial H}{\partial z} \rho_o \chi + \gamma g H \rho_o \frac{\partial \chi}{\partial z} + \gamma g H \chi \frac{\partial \rho_o}{\partial z}$$

$$- (\gamma - 1) J \frac{\partial \rho_o}{\partial z} - (\gamma - 1) \rho_o \frac{\partial J}{\partial z} - \omega g \frac{\partial \rho_o}{\partial z}$$

$$+ g w \frac{\partial \rho_o}{\partial z} + g \rho_o \chi - \rho_o \frac{\partial}{\partial t} \frac{\partial \Omega}{\partial z},$$

which may be rearranged to show

$$\frac{\partial w}{\partial z} = \gamma H \frac{\partial \chi}{\partial z} - (\gamma - 1) \chi - \frac{\gamma - 1}{g \rho_o} \frac{\partial}{\partial z} J_o - \frac{1}{g} \frac{\partial}{\partial t} \frac{\partial \Omega}{\partial z}. \tag{3.16}$$

By taking the derivative of (3.15) with respect to height

$$\frac{\partial \chi}{\partial z} - \frac{\partial^2 w}{\partial z^2} = F\left(\frac{\partial}{\partial z} \frac{\delta P}{\rho_o} + \frac{\partial \Omega}{\partial z}\right)$$

and (3.16) with respect to height

$$\frac{\partial^2 w}{\partial z^2} = \gamma \frac{\partial H}{\partial z} \frac{\partial \chi}{\partial z} + \gamma H \frac{\partial^2 \chi}{\partial z^2} - (\gamma - 1) \frac{\partial \chi}{\partial z}$$

$$- \frac{(\gamma - 1)}{g} \frac{\partial}{\partial z} \left(\frac{1}{\rho} \frac{\partial}{\partial z}\left[J \rho_o\right]\right) - \frac{1}{g} \frac{\partial}{\partial t} \left(\frac{\partial^2 \Omega}{\partial z^2}\right)$$

and by neglecting the term involving $\partial^2\Omega/\partial z^2$, $\partial^2 w/\partial z^2$ can be eliminated to yield

$$H\frac{\partial^2\chi}{\partial z^2} + \left(\frac{\partial H}{\partial z} - \frac{(\gamma-1)}{\gamma} - 1\right)\frac{\partial\chi}{\partial z} - \frac{\gamma-1}{\gamma g}\frac{\partial}{\partial z}\left(\frac{1}{\rho_o}\frac{\partial(J\rho_o)}{\partial z}\right)$$

$$= \frac{F}{\gamma}\left(\frac{\partial\left(\frac{\delta P}{\rho_o}\right)}{\partial z} + \frac{\partial\Omega}{\partial z}\right). \qquad (3.17)$$

Consider now only the term on the right hand side of (3.17). From (3.3)

$$\frac{F}{\gamma}\left(\frac{\partial\left(\frac{\delta P}{\rho_o}\right)}{\partial z} + \frac{\partial\Omega}{\partial z}\right) = \frac{F}{\gamma}\left\{\frac{-g\delta\rho - \rho_o\frac{\partial\Omega}{\partial z}}{\rho_o} - \frac{\delta P}{\rho_o^2}\frac{\partial\rho_o}{\partial z} + \frac{\partial\Omega}{\partial z}\right\}$$

and from (3.4) and 3.7)

$$\delta\rho = \frac{1}{i\sigma}\left\{-w\frac{\partial\rho_o}{\partial z} - \rho_o\chi\right\}$$

$$\delta P = \frac{1}{i\sigma}\left\{-\gamma gH\rho_o\chi + (\gamma-1)\rho_o J + w\rho_o g\right\},$$

then, where $\varkappa = (\gamma-1)/\gamma$,

$$\frac{F}{\gamma}\left(\frac{\partial\left(\frac{\delta P}{\rho_o}\right)}{\partial z} + \frac{\partial\Omega}{\partial z}\right) = -\frac{F}{i\sigma}\left\{g\chi\left(\varkappa + \frac{\partial H}{\partial z}\right) - \varkappa\left(1 + \frac{\partial H}{\partial z}\right)\frac{J}{H}\right\}, \qquad (3.18)$$

(3.17) then becomes

$$H\frac{\partial^2\chi}{\partial z^2} + \left(\frac{\partial H}{\partial z} - 1\right)\frac{\partial\chi}{\partial z} - \frac{\varkappa}{g}\frac{\partial}{\partial z}\left[\frac{\partial J}{\partial z} - \frac{1}{H}\left(1 + \frac{\partial H}{\partial z}\right)J\right]$$

$$+ \frac{F}{i\sigma}\left\{g\chi\left(\varkappa + \frac{\partial H}{\partial z}\right) - \varkappa\left(1 + \frac{\partial H}{\partial z}\right)\frac{J}{H}\right\} = 0. \qquad (3.19)$$

Equation (3.19) can be solved by the method of separation of variables. For this purpose χ and J are represented by series expansions in terms of eigenfunctions $\Psi(\theta, \varphi)$ of the operator F:

$$\chi = \sum_j \chi_j(z)\, \Psi_j(\theta,\varphi)\, e^{i\sigma t}$$

$$J = \sum_j J_j(z)\, \Psi_j(\theta,\varphi)\, e^{i\sigma t}$$

Substituting χ and J from above results in

$$H\frac{\partial^2\chi}{\partial z^2} + \left(\frac{\partial H}{\partial z} - 1\right)\frac{\partial\chi}{\partial z} - \frac{\kappa}{g}\frac{\partial^2 J}{\partial z^2} + \frac{\kappa}{g}\frac{\partial}{\partial z}\left\{\left(1 + \frac{\partial H}{\partial z}\right)\frac{J}{H}\right\}$$
$$= \frac{g}{i\sigma\Psi}\left\{\underline{-\left(\kappa + \frac{\partial H}{\partial z}\right)\chi + \frac{\kappa}{g}\left(1 + \frac{\partial H}{\partial z}\right)\frac{J}{H}}\right\} F(\Psi) \qquad (3.20)$$

where the subscripts j have been omitted from χ, J, and Ψ for convenience. If the underlined part of (3.20) is moved to the left hand side of the expression, the terms involving χ and J are separated from those containing Ψ. The new left part of (3.20) then equals $\frac{1}{i\sigma}\frac{F(\Psi)}{\Psi}$ which must in turn be equal to some constant (1/hg). Thus, a set of two ordinary differential equations result. These are:

$$F(\Psi) - i\sigma\,\Psi/gh = 0 \qquad (3.21)$$

and

$$H\frac{d^2\chi}{dz^2} + \left(\frac{dH}{dz} - 1\right)\frac{d\chi}{dz} + \left(\kappa + \frac{dH}{dz}\right)\frac{\chi}{h}$$
$$= \frac{\kappa}{g}\left[\frac{d^2J}{dz^2} - \frac{d}{dz}\left\{\left(1 + \frac{dH}{dz}\right)\frac{J}{H}\right\} + \frac{1}{h}\left(1 + \frac{dH}{dz}\right)\frac{J}{H}\right. \qquad (3.22)$$

Again the subscript j was omitted from χ, Ψ, J, and h for convenience; (3.22) is subject to further separation.

The above two expressions differ from those derived by Seibert (1961) for the non-viscous atmosphere only in the form of the operator F. Equation (3.21) is a form of Laplace's tidal equation (Craig, 1965). The other is sometimes referred to as the radial equation. To solve the set

of equations, Laplace's equation is solved for h for the particular mode of interest. The resultant h is used then in the radial equation for its solution. The addition of the height dependent viscous term to the set of tidal equations, as done here, makes it difficult if not impossible to find a general analitical solution to the set. However, some information of the effect of viscosity on the tidal wind field may be obtained from this derivation. This is more easily demonstrated in cartesian coordinates. In this system the operator F may be written as

$$\frac{f\left(\frac{\partial^2}{\partial y^2} - \frac{\partial^2}{\partial x^2}\right) - 2S \frac{\partial^2}{\partial x \partial y}}{f^2 + S^2}$$

where y is directed to the north,

x is directed to the east, and

S retains its original definition.

If values of n and σ representative of the semidiurnal tidal winds, and values of K, $\partial K/\partial z$, and $\left(\frac{1}{\rho} \frac{\partial \rho}{\partial z}\right)$ representative of the region near 100 km are inserted into the definition of S,

$$S \equiv i \left[\sigma - n\, \partial K/\partial z - Kn \left(\frac{1}{\rho} \frac{\partial \rho}{\partial z}\right)\right] + n^2 K$$

it is estimated numerically as

$$S = i \left\{\left[(1.45 - .15 + .20)\right] + .15\right\} \times 10^{-4} \text{sec}^{-1}$$

For the case where K = 0, the above becomes

$$S = \left(1.45\, i\right) \times 10^{-4} \text{sec}^{-1}$$

Thus introduction of viscosity has increased the imaginary part of S by about 4 per cent and increased the real part from zero to 0.14×10^{-4} sec^{-1}.

The significance of this effect can be demonstrated by

considering (3.2) in cartesian co-ordinates

$$v = \frac{f \frac{\partial}{\partial y} - S \frac{\partial}{\partial x}}{f^2 + S^2} \left(\frac{\delta P}{\rho_o} + \Omega \right) . \tag{3.23}$$

Where $\frac{\partial}{\partial y} \left(\frac{\delta P}{\rho_o} + \Omega \right) = 0$, i.e., the gradient is directed to the east along positive (x),

$$v = \frac{-S \frac{\partial}{\partial x}}{f^2 + S^2} \left(\frac{\delta \rho}{\rho_o} + \Omega \right) . \tag{3.24}$$

At 45^o latitude, for the values of S without viscosity,

$$v = (1.32\ i) \times 10^4 \frac{\partial}{\partial x} \left(\frac{\delta P}{\rho_o} + \Omega \right) ,$$

and when viscosity is considered

$$v = (1.04 + .49i) \times 10^4 \frac{\partial}{\partial x} \left(\frac{\delta P}{\rho_o} + \Omega \right) .$$

Thus the introduction of viscosity has brought about a change in relationship of phase between tidal wind and tidal potential. In this particular case it has advanced the phase of the wind component by about 60 degrees relative to the potential gradient.

The change in S caused by the introduction of viscosity, for the particular values used, results in a change in the operator F from

$$\left[-.91 \left(\frac{\partial^2}{\partial y^2} - \frac{\partial^2}{\partial x^2} \right) + 1.45\ i \frac{\partial^2}{\partial x\, \partial y} \right] \times 10^{-4}$$

for the case without viscosity to

$$\left[-.72 \left(\frac{\partial^2}{\partial y^2} - \frac{\partial^2}{\partial x^2} \right) - .56 \frac{\partial^2}{\partial x\, \partial y} + i \left\{ -.26 \left(\frac{\partial^2}{\partial y^2} - \frac{\partial^2}{\partial x^2} \right) + 2.24 \frac{\partial^2}{\partial x\, \partial y} \right\} \right] \times 10^{-4}$$

when viscosity is introduced. This change in F must result in a

corresponding change in the series of h in (3.21) and hence changes the solutions for (3.22).

Subsequent chapters discuss certain of the effects of viscosity on the tidal winds in somewhat greater detail. However the numerical approaches used in this paper to perform the tasks discussed in Chapter I differ in many ways from an attempt to solve (3.21) and (3.22). These derivations were presented to show where the viscous terms entered the tidal equations and to show they were of significant magnitude to warrant consideration.

CHAPTER IV

EDDY VISCOSITY IN THE ATMOSPHERE

The physical aspects of molecular and eddy viscosity differ in several ways. In molecular processes, momentum is transferred in an instantaneous collision. In the eddy process this transfer is prolonged in both time and space. For the atmosphere, the molecular coefficient of viscosity is completely dependent on temperature, over the normal range of temperature. In the eddy process, factors such as static stability, composition differences, wind shears and roughness parameters are of greater importance in determining the "coefficient of eddy viscosity". In the atmosphere, except at the atmosphere-surface interface and above about 115 km altitude, the eddy effects are usually much greater than the molecular terms, and they often vary a great deal in time and space. The magnitude of this variation is still not predictable, even in the lower few hundred meters.

To handle the eddy viscosity effects with some semblance of order and mathematical simplicity, an analogy can be made to the molecular processes, known as Prandtl's Theory (Haltiner and Martin, 1957). By assuming that parcels of air behave as molecules, the investigator is able to observe the effects of the eddy process, and to determine the magnitude of the molecular process required to achieve the same results. This ficticious value is then referred to as the eddy coefficient.

The coefficient of molecular viscosity (μ) then is analogous to the eddy exchange (Austausch) coefficient (A) and the coefficient of kinematic viscosity ($\eta \equiv \mu/\rho$) is analogous to the eddy diffusion coefficient ($K \equiv A/\rho$). The latter is often referred to as the coefficient of eddy viscosity. There is another significant difference between η and K. In the molecular case, there is a general trend towards uniformity of the coefficient in all directions; however, K may differ greatly between its horizontal and vertical components. For systems of large horizontal scale, however, the gradients of the parameters to be transported are usually so much greater in the vertical than in the horizontal, the net vertical flux usually dominates (Haltiner and Martin, 1957).

In this paper two effects of eddy viscosity are considered. The major emphasis is placed on the vertical transfer of momentum, but the viscous heating brought about by the dissipation of momentum is also considered.

The action of viscosity serves to convert kinetic energy to thermal energy. Thus, the overall kinetic energy of a closed system would be reduced. Individual elements of the fluid within such a closed system can increase their kinetic energy during this decay process, however, provided the distribution of momentum in the fluid meets certain requirements.

As an example, consider the case where the wind at the base is zero and velocity increases with altitude. The acceleration on individual elements in the fluid due to the action of viscosity (shear stress) is

$$\frac{\partial u}{\partial t} = \frac{1}{\rho}\left[\frac{\partial}{\partial z}\left(\rho K \frac{\partial u}{\partial z}\right)\right] . \qquad (3.25)$$

If u is positive and the term in brackets is positive, the momentum per unit mass of an individual element is increased. Had the term in parenthesis been negative, the kinetic energy of the elements would decrease, and if the term is zero no change would occur. Thus for the singular case of no change

$$\frac{\partial}{\partial z}\left(\rho K \frac{\partial u}{\partial z}\right) = 0; \quad \rho K \frac{\partial u}{\partial z} = \text{constant}. \tag{4.26}$$

Dividing by ρK and integrating from some level designated as the base ($z_o = 0$) to some level above (z), we get

$$\int_{u_o}^{u} du = \int_{z_o}^{z} (\text{const}) \frac{dz}{\rho K} . \tag{4.27}$$

If we let both ρ and K be dependent on z such that $\rho = \rho_o e^{bz}$ and $K = K_o e^{cz}$, where b is defined so that ρ (z) approximates the standard atmosphere (COESA, 1962) and c is defined so that K (z) approximates the vertical distribution of K as given by Johnson and Wilkins (1965b), then the above expression becomes

$$\int_{u_o}^{u} du = \int_{z_o}^{z} \frac{(\text{constant})\ (dz)}{\rho_o K_o e^{(b+c)z}} . \tag{4.28}$$

The constant is defined by known values of ρ_o, K_o and $\left(\frac{\partial u}{\partial z}\right)_o$ so that

$$\int_{u_o}^{u} du = \int_{z_o}^{z} \frac{\rho_o K_o \left(\frac{\partial u}{\partial z}\right)_o dz}{\rho_o K_o e^{(b+c)z}} = \left(\frac{du}{dz}\right)_o \int_{z_o}^{z} e^{-(b+c)z} dz. \tag{4.29}$$

and

$$u = u_o - \frac{+\left(\frac{\partial u}{\partial z}\right)_o}{b+c} \left[e^{-(b+c)z} - 1 \right], \tag{4.30}$$

Now for the portion of the standard atmosphere under consideration in this paper $|b| > |c|$ with b negative ($-1.57 \times 10^{-4} m^{-1}$) and c positive ($1.11 \times 10^{-4}\ m^{-1}$) so that

$$u = u_o + 13220\ (\partial u/\partial z)_o \left[e^{.0000756\ z} - 1\right], \tag{4.31}$$

Figure 4 shows the profile of wind required for zero acceleration due to viscosity for $(\partial u/\partial z)_o$ arbitrarily defined at 0.001 sec^{-1}. Should the curvature of the wind profile be greater than shown, individual elements of air will experience an increase in kinetic energy. While the discussion above is for an unbounded system, obviously inappropriate for the atmosphere for the wind will not increase without bounds, transient periods do exist in which increases in the kinetic energy of individual elements are brought about due to the effects of viscosity.

As shown by Lamb (1932), the expression

$$\mu \left\{ 2\left(\frac{\partial u}{\partial x}\right)^2 + 2\left(\frac{\partial v}{\partial y}\right)^2 + 2\left(\frac{\partial w}{\partial z}\right)^2 + \left(\frac{\partial w}{\partial y} + \frac{\partial v}{\partial z}\right)^2 + \left(\frac{\partial u}{\partial z} + \frac{\partial w}{\partial x}\right)^2 + \left(\frac{\partial v}{\partial x} + \frac{\partial u}{\partial y}\right)^2 \right\}$$

represents the rate at which mechanical energy is disappearing due to the action of molecular viscosity. This energy takes the form of heat in the element.

For the condition considered in this paper, where all other terms are small compared to the vertical shear of the horizontal wind, the heating terms are reduced to

$$\mu \left[\left(\frac{\partial v}{\partial z}\right)^2 + \left(\frac{\partial u}{\partial z}\right)^2 \right] .$$

The temperature change experienced by a unit volume per unit time then is

$$\frac{\partial T^*}{\partial t} = \mu \left[\left(\frac{\partial v}{\partial z}\right)^2 + \left(\frac{\partial u}{\partial z}\right)^2 \right] / \mathcal{J} c_p \rho \qquad (4.32)$$

where

$\mathcal{J}$ is the mechanical equivalent of heat, and

c_p is specific heat of air at constant pressure.

An analogy between the effects of molecular and eddy viscosity in the viscous heating terms is not so obvious as the analogy between the effects of these parameters in the process of momentum transfer. It is quite easy to visualize an element in a shearing field being displaced into a region where the ambient velocity differs from the velocity of the element, with a resulting momentum transfer. However, such a displacement will also produce a field of shear about the element which is much greater than the initial shearing field, hence a greater degree of heating will result. Thus, where eddy viscosity terms are much greater than the molecular terms the heating resulting from the eddy motions will be correspondingly higher than those due to purely molecular effects.

The values for the coefficient of eddy viscosity (K) used later on in this paper are those deduced by Johnson and Wilkins (1965b), or values along a smooth curve approximating the curve deduced by these investigators. Where other values are used they are referred to in terms of the values along the smoothed curve. The smoothed curve actually overestimates the values of K given by Johnson and Wilkins over most of the altitude range. It does agree with the value at 85 km and with the vertical gradient of K near 100 km.

Johnson and Wilkins arrived at the height distribution of mean maximum values of eddy viscosity by determining the value required to

maintain a steady state temperature profile (that of the U. S. Standard Atmosphere, 1962) in the presence of absorption of solar radiation. These calculations required several assumptions. The heating of this region due to viscous dissipation of internal gravity waves, tides and turbulent eddies was assumed small compared to solar heating, as were the infrared heat losses above 90 km. Infrared flux was assumed to be 15% of the total heat input between 60 and 90 km. It was further assumed that the chemical energy available as a result of downward flux of molecular oxygen to regions below 85 km, where it rapidly combines in a three-body process, all appeared eventually as heat, although it was realized that a small fraction appeared as airglow.

The flux of heat due to turbulent mixing may be expressed as

$$F_{\downarrow} = -c_p \rho K_T T^* (\partial \theta^* / \partial z) / \theta^* \qquad (4.33)$$

where

K_T is the coefficient for eddy diffusion of heat (assumed equal to K),

T^* is temperature, and

θ^* is potential temperature.

Since $F_{\downarrow}$ is determined by considering the steady state temperature and heat input as a function of altitude, K_T is readily determined. This calculation maximizes K_T since it represents a transfer downward of all the heat available.

There is some indication from mass spectrometer measurements of the O to O_2 concentration ratio above 100 km (Colegrove et al, 1965) that the average K must be about one half that of the average value of K maximum. Justus (1967) used wind profile and turbulent wind data

obtained by tracking of rocket released chemical clouds to compute thermal and momentum eddy diffusivities in the 90 to 110 km region. Relatively good agreement exists between his value of K and that determined by Johnson and Wilkins. A comparison of these different computations of K is shown in Figure 5.

Hines (1965) has calculated the heating rate due to viscous dissipation of internal gravity waves and has suggested that it may equal solar heating at about 120 km. By considering the rate of decay of tidal energy with height he deduced that heating by viscous dissipation of tidal energy to be of similar magnitude. Heating due to the viscous action on tides, however, is insignificant compared to that due to absorption of solar energy as calculated by Johnson and Wilkins throughout the altitude range considered here.

CHAPTER V

MODELING THE EFFECTS OF VISCOSITY ON TIDAL SCALE MOTIONS IN THE UPPER MESOSPHERE AND LOWER THERMOSPHERE

A description of the effects of viscosity and Coriolis force on atmospheric motions is presented before the models are developed to demonstrate certain features which may be easily overlooked in the models themselves.

The effects of viscosity and Coriolis force on tidal scale motions will be examined in the following chapters, first by considering each effect separately on initial wind distributions; then the combined effects of these forces, again acting on an initial wind distribution, is considered. Finally a forcing function is introduced, and the models of the semidiurnal tidal wind field near the mesopause are evolved. The terms which will be examined appear in the set of equations for tides, as derived in Chapter III, as important ones for modifying tidal motions for the region of interest. As noted earlier the terms responsible for origination of tidal motions have been investigated extensively by others. Ideally, the influence of viscosity and Coriolis force should be studied by taking these terms into account. However for simplicity, and because of the questions which remain concerning tidal origin, a hypothetical tidal oscillating similar to the observed semidiurnal tide in the region of interest and in general agreement with tidal theory as developed by

Seibert (1961), is generated. The models presented here will be concerned only with the modification or contribution the effects of viscosity have on this oscillation. Complexities introduced by using a coefficient of eddy viscosity which is permitted to vary in time and height discourage any attempt to apply an analytic approach to the models. Two simplifying assumptions are used throughout. First, only the vertical component of the coefficient of eddy viscosity is considered. This assumption should have little effect on the results since horizontal shears are usually much smaller than those in the vertical. Secondly, the local and total derivatives are assumed identical. This is also common practice when considering wave motion where the velocity of the perturbation greatly exceeds the velocity of individual elements of air.

First, consider a hypothetical atmosphere similar in vertical structure to the earth's mesosphere, and which is motionless, except for a sine-form perturbation in the vertical distribution of horizontal wind. To avoid the problem of a boundary, let there be an infinite number of oscillations in the vertical, all initally of equal amplitude (Fig. 6). The acceleration of an individual element of air at some height due to motion at a different height, transmitted to it by the effects of eddy viscosity, as expressed by (3.17) is

$$\frac{\partial u}{\partial t} = \frac{1}{\rho} \frac{\partial}{\partial z} \left(\rho K \frac{\partial u}{\partial z}\right).$$

Arbitrarily taking values typical of the mesosphere between 70 and 82 km for ρ as determined from the 1962 U.S. Standard Atmosphere (COESA, 1962) and K from Johnson and Wilkins (1965a,b), determination can be made of the changes in the velocity profile resulting from viscosity. The values

actually used here for K are the maximum values (smoothed) as determined by Johnson and Wilkins. While ρ decreases logarithmically with height, K experiences a logarithmic increase with height in the region of interest. Define

$$K \equiv K_o e^{cz}$$

$$\rho \equiv \rho_o e^{bz}$$

and let

$$u_o = U_o \sin(2\pi z/L)$$

where

u_o is the initial perturbation,

U_o is the initial perturbation amplitude, and

L is the vertical wavelength of the perturbations.

U, of course, is time dependent, but since here we will be concerned only with the accelerations near the initial conditions, the dependence will be neglected. Substituting the above expression into (4.25), we arrive at

$$\left.\frac{\partial u}{\partial t}\right)_{t=0} = K_o U_o e^{cz} \left[(b + c)\,\frac{2\pi}{L} \cos\frac{2\pi}{L} z - \frac{4\pi^2}{L^2} \sin\frac{2\pi}{L} z\right] .$$

Consider point 1 in Fig. 6 as being at z = 0. Here the curvature in the vertical profile of wind is zero, and the point at first glance would be expected to experience no acceleration due to viscosity; however, because of the variation of ρ and K with altitude, an acceleration is experienced equal to $K_o U_o e^{cz}$ (b+c) $2\pi/L$. Thus, point 1 experiences a negative acceleration. The point of zero acceleration lies somewhat below point 1. Point 2 experiences a positive acceleration equal to $K_o U_o e^{cL(b+c)/2}$ $2\pi/L$. There is then an upward propagation of this wind pattern accompanying its

decay. It is interesting to note that the acceleration at the points of no wind, increase upward according to the exponential e^{cz}. In order to get a downward propagating wind pattern due to viscosity under the conditions established, $|c|$ must be greater than $|b|$. It is difficult to say if such conditions ever exist; however, if they do, a preferred region would be in the lower thermosphere where, if we let c define the rate of growth of the cumulative effects of eddy and molecular viscosity, these combined effects could possibly exceed the effects of the decay of density with height. However, in this region b is also quite large.

It is mathematically possible for the propagation coefficient $(c+b)2\pi/L$ to be greater than the dissipation coefficient $4\pi^2/L^2$. However, this would require that $L > 2\pi/(b+c)$, and for the values of b and c common to the mesosphere ($c=1.11 \times 10^{-4}$; $b=-1.57 \times 10^{-4}$ between 70 and 82 km) this would require $L > 130$ km, a ridiculously large value.

It is of interest to consider how viscosity might affect the propagation of kinetic energy. To do this it is preferred that a more realistic perturbation (one of finite extent) be adopted. Fig. 7 depicts such a perturbation, symmetrical about its maximum velocity. At points 1 and 2, let the velocity, the vertical shear and curvature of the horizontal wind profile be equal and denote the shear as Q. Retaining the definition of K and ρ with height, the accelerations at these points are found to be:

$$\frac{\partial u}{\partial t} = K_o e^{cz} \left[\frac{\partial Q}{\partial z} + (b + c)\, Q\right], \tag{5.34}$$

The ratio of the acceleration at point 2 to that at point 1 is e^{cz} (equals 3.83 between 70 and 82 km). Since kinetic energy (K.E.) is $\rho v^2/2$, and

$\partial(K.E.)/\partial t$ is $\rho v \partial v/\partial t$ if $\partial\rho/\partial t = 0$. The ratio of change of K.E. with time at point 2 to point 1 is

$$\frac{\rho_2}{\rho_1} e^{cz},$$

where z is the distance between points 1 and 2. For the region between 70 and 82 km this ratio is 0.605. That is, while a general diffusion of the K.E. of the initial perturbation is apparent and the increase in velocity is greater at point 2 than at point 1, more of the K.E. is directed downward than upward.

Recall that the above discussion is only valid near the initial time. The variation of viscosity and density with height will bring about significant changes in shape of the wind profile in time for the conditions decribed here. The tidal wind field, of course, represents a balance between this loss of energy and the tidal energy input. For the particular case where ρK is independent of height (4.25) becomes

$$\frac{\partial u}{\partial t} = K \frac{\partial^2 u}{\partial z^2} , \tag{5.35}$$

and

$$u = Ue^{(-n^2Kt + inz)} \tag{5.36}$$

is a solution. We see that $\frac{1}{u}\frac{\partial u}{\partial t} = -Kn^2$, that is, the per cent of velocity decay per unit time for n = 2 is four times that for n = 1. Thus shorter wavelength oscillations are rapidly damped relative to the longer wavelengths. As an example near the mesopause (assume K is 1000 m^2/sec) the half life of a oscillation with vertical wavelength of 50 km is about 12.3 hours but for one of 5 km only about 8 minutes. It is also possible to obtain a general solution to (4.25) by again letting $\rho = \rho_o e^{bz}$ and $K = K_o e^{cz}$; (4.25) then becomes

$$\frac{\partial u}{\partial t} = K_o e^{cz} \left(\frac{\partial^2 u}{\partial z^2} + (b + c) \frac{\partial u}{\partial z}\right). \tag{5.37}$$

Assuming a solution of the form $u = Z(z)T(t)$ and separating variables gives

$$\frac{1}{T}\frac{\partial T}{\partial t} = \frac{K_o e^{cz}}{Z}\left[\frac{\partial^2 Z}{\partial z} + (b + c)\frac{\partial Z}{\partial z}\right] = -\lambda^2 , \tag{5.38}$$

where $-\lambda^2$ is the separation constant. The decay equation is

$$T = T_o e^{-\lambda^2 t}, \tag{5.39}$$

and the equation of Z may be written as

$$\frac{\partial^2 Z}{\partial z^2} + (b + c)\frac{\partial Z}{\partial z} + \frac{\lambda^2 e^{-cz} Z}{K_o} = 0 \tag{5.40}$$

This reduces to one of the standard forms of Bessel's equation having a functional solution of the first kind. This can be shown if we use the transformation

$$x = e^{-cz};\ Z = y(x),$$

where

$$\frac{d}{dz} = \frac{d}{dx}\frac{dx}{dz} = -cx\frac{d}{dx},$$

and therefore (5.40) becomes

$$x\frac{d^2 y}{dx^2} - \frac{b}{c}\frac{dy}{dx} + \frac{\lambda^2 y}{c^2 K_o} = 0, \tag{5.41}$$

which has the solution, given by Kamke (1948),

$$y = x^{\left(\frac{b+c}{2c}\right)} \mathcal{Z}_\nu (\lambda X) \tag{5.42}$$

where

$\mathcal{Z}_\nu = c_1 J_\nu + c_2 J_{-\nu}$; c_1 & c_2 are arbitrary,

$\nu = 1 + b/c$, and $\lambda X = (4\lambda^2 x/c^2 K_o)^{\frac{1}{2}}$.

Reverting to the original variables we have

$$Z = \left[e^{(b + c)z/2}\right] \mathcal{Z}_\nu \left[\left(4\lambda^2 e^{-cz}/c^2 K_o\right)^{\frac{1}{2}}\right] \tag{5.43}$$

A complete solution then is of the form

$$u = \sum_{n=1}^{\infty} T_o \exp[(b + c)z/2 - \lambda_n^2 t][A_n J_\nu(\lambda_n X) + B_n J_{-\nu}(\lambda_n X)], \tag{5.44}$$

The complexity of this expression over (5.36) is required to permit the vertical propagation of the initial waveform due to variation of ρK with height. The coefficients in (5.44) may be solved for defined initial conditions. The expression does not, however, permit K to be time dependent.

The final consideration of viscosity separately involves the development of a numerical approach. Consider an atmosphere similar to the mesosphere in its vertical structure, its upper terminal point (i.e., boundary) being at 90 km. The distribution of the coefficientof eddy viscosity with height is again taken as the maximum value as derived by Johnson and Wilkins. The upper boundary is forced to move back and forth in a manner similar to that of the semidiurnal tide as observed by Greenhow and Neufeld (1955), except that here only a single component of motion is considered. The vertical increment in the finite difference scheme is 1 km and the time increment is 150 seconds with a printout of velocity as a function of height for each hour. The initial condition was without net motion ($u = 0$) and the model was allowed to run for 25 hours. While the top boundary was driven by acceleration of cosine form of period of 12 hours, the only horizontal acceleration experienced by the lower layers are due to the action of eddy viscosity. The finite difference expression for the acceleration (from 3.17) at point n is

$$\frac{du}{dt}_{(n)} = \frac{1}{\rho_{(n)}\Delta z^2}\left[K_{(n+1/2)}\rho_{(n+1/2)}\left(u_{(n+1/2)} - u_{(n)}\right)\right.$$
$$\left. -K_{(n-1/2)}\rho_{(n-1/2)}\left(u_{(n)} - u_{(n-1/2)}\right)\right], \qquad (5.45)$$

where n represents the number of the specified height as n increases upward; and the expression for velocity after time increment Δt is

$$u_{(t_o+\Delta t)} = u_{(t_o)} + \frac{du}{dt}\Delta t. \qquad (5.46)$$

The requirements for computational stability for the forward time steps used in this calculation for the case where ρ and K are independent of height was tested numerically in (5.45) and (5.46) and were found to be satisfactory. This requirement as given by Richtmyer (1957) is

$$\frac{K\Delta t}{(\Delta z)^2} = \text{constant} \leq 1/2, \qquad (5.47)$$

For the largest value of K used (2493 m^2/sec) and the height interval used (1000 m), $\Delta t \leq 200$ seconds. The time interval actually used in this and all other calculations was 150 seconds.

Truncation error was detectable (about 2.5 per cent after 12 hours of operation) in this calculation. In the models described later it was found, by trial, that this error could be reduced to the point that it was undectable after 24 hours to two decimal places in a field of four digits if u was multiplied by a corrective factor (0.99984) after each iteration.

Equations (5.45) and (5.46) used in the above manner describe a condition analogous to standing on a platform and holding a rope over the side, with the density of the rope increasing downward as does its

flexibility except that only viscosity is the restoring force here. As the upper end of the rope is waved back and forth a wave form is generated. The amplitude of this waveform is seen to decrease with distance from the origin, in part because of the increased density of the rope and in part because of the transfer of kinetic energy into thermal energy. Because of the increased flexibility downward, the wavelength of the perturbation would also decrease.

Some of the results of the numerical approach are shown in Fig. 8 and Fig. 9. Fig. 8 depicts the wave forms at 1 hour, 8 hours, 12 hours and 25 hours after the initial time for an atmosphere where K was defined according to Johnson and Wilkins. Note the 12 hour curve indicates a half wavelength of about 4 km. Some indication of the error introduced by the finite difference method is apparent here, since at 12 hours the topmost point is not quite at its initial position. The amplitude of the perturbation becomes quite small by the time it has penetrated to 84 km. But a printout of the kinetic energy does indicate, even here, that the downward propagation of energy continues. Also of interest in Fig. 8 is that the vertical distance between maximum and minimum velocity at 8 hours is about 3 km. Had this atmosphere been allowed to continue above 90 km with the driving level remaining at 90 km, the pattern above would be similar to that below, except the wavelength and distance from maximum to minimum velocity would be increased due to the increase in eddy viscosity with height. To determine how such an increase in viscosity would affect the wave form, the viscosity as used in arriving at Fig. 8 was doubled and the results are shown in Fig. 9. The most significant difference between the two figures is the increased wavelength and depth of

penetration of the perturbation.

The Contribution of the Coriolis Force to Tidal Motions

In spite of their fictitious nature, the Coriolis effects can result in apparent vertical phase propagation of existing wave forms. To point out this phenomenon, an expression is derived which includes the effects of both Coriolis and viscous terms. A model is constructed containing a wave form as the initial condition, and in one case the viscous term will be permitted to approach zero.

Consider the equations of motion for a homogeneous atmosphere in which advection and pressure gradient can be neglected. The coefficient of eddy viscosity is assumed independent of height, i.e.,

$$\frac{\partial u}{\partial t} = fv + K \frac{\partial^2 u}{\partial z^2} \tag{5.48}$$

$$\frac{\partial v}{\partial t} = -fu + K \frac{\partial^2 v}{\partial z^2} \, . \tag{5.49}$$

Let initial conditions be

$$u_{(t=0)} = A_{1_{(t=0)}} \sin \frac{2\pi z}{L} \tag{5.50}$$

$$v_{(t=0)} = A_{2_{(t=0)}} \sin \frac{2\pi}{L}(z - D) \tag{5.51}$$

where,

A_1 is the amplitude of the u component of velocity,

A_2 is the amplitude of the v component of velocity,

L is the vertical wavelength of the perturbation, and

D is the displacement of phase of v from u.

Substituting the initial conditions into (5.48) and (5.49), we get for

initial time

$$\left.\frac{\partial A_1}{\partial t}\right|_{t=0} \sin\frac{2\pi z}{L} = fA_2 \sin\frac{2\pi}{L}(z - D) - KA_1\frac{4\pi^2}{L^2}\sin\frac{2\pi}{L}z \qquad (5.52)$$

$$\left.\frac{\partial A_2}{\partial t}\right|_{t=0} \sin\frac{2\pi}{L}(z - D) = -fA_1 \sin\frac{2\pi}{L}z - KA_2\frac{4\pi^2}{L^2}\sin\frac{2\pi}{L}(z - D), \qquad (5.53)$$

Rearrangement of (5.52) results in

$$\frac{\left.\frac{\partial A_1}{\partial t}\right|_{t=0} + KA_1\frac{4\pi^2}{L^2}}{fA_2} = \frac{\sin\frac{2\pi}{L}(z - D)}{\sin(\frac{2\pi}{L}z)} \qquad (5.54)$$

With (5.54) discussion of the effects of phase difference between the two components of motion is simplified. For the sake of discussion let $z = L/4$ so that the denominator on the right is one. The terms $KA_1 4\pi^2/L^2$ and fA_2 are always positive. For $D = L/2$, the right hand side of (5.43) is -1, that is, $\partial A_1/\partial t$ is at its largest negative value. For $D = \pm L/4$, the right side of (5.43) is zero and $\partial A_1/\partial t$ is still negative but now is independent of the Coriolis force. When $D = 0$ however, the right hand side of (5.43) is +1 and now $\partial A_1/\partial t$ may be either positive or negative depending on the relative magnitude of the other terms. For the atmosphere near the mesopasue in middle latitudes the Coriolis term is the larger for wavelengths of the semidiurnal tide thus $\partial A_1/\partial t > 0$. Returning to consideration of the case where $D = L/4$, which is the observed case for the semidiurnal tide near the mesopause, at $z = L/2$, u and $\partial^2 u/\partial z^2$ are zero from (5.50) and v is at its maximum value; (5.48) then shows $\left.\frac{\partial u}{\partial t}\right|_{t=0} = f A_2$. The meaning of these results is better seen in graphical form. Fig. 10 shows the components of velocity u as a solid line, v as a dashed line with v being displaced by L/4 from u. Fig. 11 shows the components displaced by L/2. The relative accelerations are

denoted by arrows. By considering the equation of motion and retaining only the Coriolis term

$$\frac{\partial u}{\partial t} = fv \tag{5.55}$$

$$\frac{\partial v}{\partial t} = -fu \tag{5.56}$$

it is readily apparent that each component of motion acts upon the other, but the apparent result of this action is dependent on the phase difference between the components. In Fig. 10 there is no apparent change in amplitude of either component with time, but there is an apparent downward propagation of both the u and v components. Had the phase difference been L/4 in the other direction, the apparent propagation would have been upward. In Fig. 11 there is no apparent propagation; instead the v component appears to grow at the expense of the u component. There is, however, no propagation of kinetic energy in either case. This can readily be demonstrated by multiplying (5.55) by u and (5.56) by v and adding the two expressions.

$$u\frac{\partial u}{\partial t} + v\frac{\partial v}{\partial t} = fvu - fvu = 0$$

Nevertheless an observer situated in the plane of one of the components, so that only the motion of the other would be apparent to him, would sense in the case of Fig. 10, the apparent wave propagation (actually an illusion similar to the revolving barber's pole), and in the case of Fig. 11, a pulsation of the visible component. The period required to return to the initial condition would be $2\pi/f$, that is, one half pendulum day. Motion of this type has been observed in the sea (Sverdrup, 1942), and it is certainly important in the atmosphere although it is

often masked by other factors. Later models show that in the semi-diurnal tide, the acceleration due to the Coriolis effect is about twice that caused by other forces near 45 degrees latitude.

Combined Action of Viscous and Coriolis Accelerations

The difference between the actions of the Coriolis or inertial wave with viscosity to the action without viscosity is seen by using the following numerical approach. The atmosphere is considered homogeneous with K independent of height. K was assumed to be 10^6 cm^2/sec (a rough estimate from Johnson and Wilkins) for the case with viscosity, and 1 cm^2/sec for the case without, and f was assumed to be 10^{-4} sec^{-1}. A comparison of the two cases can be made by referring to Fig. 12. There the initial u and v wind components are indicated by the solid lines and the "final" conditions, two hours later, are indicated by dashed lines for the case with both viscosity and Coriolis, and by a series of dots for the case of Coriolis alone. Both cases indicate the same apparent wave propagation, although it is not so obvious in this figure. There is a definite reduction in the amplitude of the v component in both cases, although the viscous case showed greater reduction. Both cases showed an increase in the u amplitude, and of course in the viscous case the increase was less than in the non-viscous case.

To test the combined effects of viscosity and Coriolis in a more realistic atmosphere, consider again the situation earlier compared to a dangling rope. This differs from the dangling rope in that only viscosity is the restoring force and Coriolis effect is of no consequence in the rope. The numerical approach remains the same except the topmost layer is now moved in a circular or elliptical pattern. Again

the amplitude and phase of the perturbation of this topmost layer is taken from the semidiurnal tidal component as resolved by Greenhow and Neufeld. The accelerations at the levels below are now the summation of the effects of viscosity and Coriolis force. The initial conditions are zero velocity in the u component and the v component decreasing at about 8 per cent per km with depth (the theoretical decrease of the tidal component as given by Hines (1960)). Again the system is allowed to operate for 25 hours. Certain of the results of this test are given in Fig. 13. Of particular interest is the graph depicting the winds 25 hours after the initial time. At this time there is a very large decrease in kinetic energy between the topmost layer at 90 km and the region 3 km below. There is also an anticyclonic turning of the winds with altitude (veering) similar to that noted by Kochanski (1964) between 83 and 133 km.

Had the model been permitted to extend above 90 km with the driving level remaining at 90 km, another point of minimum kinetic energy would be expected above the level of maximum winds but the direction of rotation of the wind would be reversed, i.e., backing with height, contrary to that noted by Kochanski. The primary objection to this model, however, is that it permits tidal accelerations to act at only a single level.

Determination of the Semidiurnal Tidal Forcing Function

The acceleration acting on each parcel of air for tidal motions are, tidal driving accelerations, viscous accelerations, and Coriolis accelerations. The tidal driving acceleration is the initiator of the motion field. Once motion begins, the Coriolis acceleration is activated and if the fluid is viscous and the motion field non-uniform, the viscous

term becomes important.

The tidal driving acceleration is the gradient of $(\frac{P}{\rho} + \Omega)$ (Ω is the gravitational potnetial). This gradient will be referred to as the tidal forcing function (TFF), in subsequent discussions. It is not the intent of this paper to delve into its origin. The Coriolis acceleration is $-\vec{f}x\vec{V}$ (always directed to the right in the northern hemisphere) and the viscous acceleration is $\frac{1}{\rho}\frac{\partial}{\partial z}(\rho K \frac{\partial v}{\partial z})$. The sum of accelerations acting on a parcel in tidal motion then, in component form, is

$$\frac{du}{dt} = fv + \frac{1}{\rho}\frac{\partial}{\partial z}(\rho K \frac{\partial u}{\partial z}) + TFF_x \tag{5.57}$$

$$\frac{dv}{dt} = -fu + \frac{1}{\rho}\frac{\partial}{\partial z}(\rho K \frac{\partial v}{\partial z}) + TFF_y \ . \tag{5.58}$$

If the wind field is known in height and time, as is assumed to be the case with tidal motions in the region of interest for a specified latitude, the TFF may be determined. This is the usual method of deducing the pressure field from the tidal wind field. However, the viscous term has not been considered in this determination in the past. This viscous term may be safely ignored in the lower atmosphere, but can offer a significant contribution in the 85 to 110 km region.

To maintain a constant amplitude periodic oscillation, the sum of all acceleration must be directed at right angles to the velocity vector. Any departure from this results in a change of phase and amplitude until eventually an equilibrium is reached in which the wind adjusts itself so that it is normal to the sum of accelerations. In the northern hemisphere, the Coriolis acceleration vector is directed to the right of the wind and in the absence of other acceleration, this would result in an inertial oscillation (period $2\pi/f$). If the sum of other accelerations

is directed along the Coriolis acceleration vector, the period of the oscillation will be reduced; if it is opposed, the period will be increased.

A model is constructed which permits the determination of the tidal forcing function vector which would exist for equilibrium in the region of interest for various values of K. The model is then amended so that it retains a realistic value of TFF and K is permitted to vary. The resultant velocities are then determined in time and space.

For the determination of TFF the model constructed was based at 85 km with its top at 110 km. The grid was spacially centered. The wind field was defined in space and time so there was no need to include a time increment. Realizing, however, that such would be required for the amended program, a forward time step (Δt = 150 sec) was included for the determination of velocity components rather than defining them in a functional form. This permitted a test of the overall program stability which proved to be excellent.

Given at the initial time (0000 or 1200 hours local time), was the wind distribution as a function of height as taken from Greenhow and Neufelf (1955). The functional expression used was

$$u(z) = u(85)\ e^{(\text{constant}_w)(z-85)} \sin\left(\varphi^*_{85} - \frac{\partial \varphi^*}{\partial z} z\right) \tag{5.59}$$

for $z \leq 100$ km and

$$u(z) = u(85)\ e^{(\text{constant}_w)(15)} \sin\left(\varphi^*_{85} - \frac{\partial \varphi^*}{\partial z} z\right) \tag{5.60}$$

above to 110 km.

A similar expression was used for v(z) except the cosine function was used.

For the constants used (u_{85} - 10 m/sec, $const_w = 0.09242\ km^{-1}$, φ^*_{85} (phase angle at 85 km) = $-5\pi/6$ and $\partial\varphi^*/\partial z = 7^o km^{-1}$), the resultant wind was a clockwise spiral in height with an exponential increase in wind speed from 10 m/sec at 85 km to 40 m/sec at 100 km. Above 100 km the spiral continued but with no increase in wind speed.

The coefficient of eddy viscosity was defined by a smooth curve approximating that given by Johnson and Wilkins (1965b) and is shown in Fig. 5. Its functional form is

$$K_{(z)} = K_{85}\, e^{c(z-85)}, \tag{5.61}$$

K_{85} was taken as 300 m^2/sec and c as 0.08318. The density distribution in height was defined as

$$\rho_{(z)} = \rho_{85}\, e^{b(z-85)} \tag{5.62}$$

with b = -0.1756 to approximate the U.S. Standard Atmosphere, 1962 (COESA, 1962).

To account for the second derivative in the viscous term another vertical grid was superimposed on the first with points midway between the basic grid points. Values of $K_{(z+\frac{1}{2})}$ and $\rho_{(z+\frac{1}{2})}$ were defined in this grid. In finite difference format the expression for u after the interval Δt is written as:

$$u_{(t_o+\Delta t)} = u_{(t_o)} + \Delta t \left[fv_{(t)} + \frac{1}{2}(TFF_{(t)} + TFF_{(t_o+\Delta t)} + [\rho_{(z+\frac{1}{2})}\, K_{(z+\frac{1}{2})}(u_{(z+1)} - u_{(z)}) - \rho_{(z-\frac{1}{2})}\, K_{(z-\frac{1}{2})}(u_{(z)} - u_{(z-1)})]/\Delta z^2 \right] \tag{5.63}$$

where TFF was defined in functional form in terms of the defined wind

distribution.

The program was designed to give the following output at initial time for a one km interval between 85 and 110 km: z, K_z, $K_{(z+\frac{1}{2})}$, $\rho_{(z)}$, $\rho_{(z+\frac{1}{2})}$, u, v, and amplitude of oscillation. At each hour thereafter, the output was: t, z, u, v, kinetic energy per unit volume, approximated Richardson number, components of acceleration due to Coriolis, TFF, and viscosity, convergence of the zonal wind, individual acceleration vector due to Coriolis, viscosity and TFF, and the acceleration vector of their sum, increase in temperature due to viscous dissipation of kinectic energy, and integrated kinetic energy.

The determination of convergence of zonal wind was made to estimate both the divergence field and the relative vertical motion field. However, to infer either of the above from the convergence of the zonal wind, an assumption must be made that probably has little basis in fact. The assumption is, the contribution of the meridional wind to convergence is zero. This does not permit a significant change of phase or amplitude of the tidal winds with latitude. Very little is known of the real latitudinal dependence of phase and amplitude, however they should certainly be great enough to make calculation of divergence based on convergence of zonal wind alone, at best, little more than a first approximation. Instead of presenting the convergence in the usual manner, the program, through the equation of continuity, determines the vertical velocity at the top of a one km slab, assuming the base of the slab is stationary. If upward velocity is indicated, convergence is occurring in the slab. The vertical velocity (w) relative to the base of the model may be determined by summing all velocities below the height of concern.

The temperature increase due to viscous dissipation of kinetic tidal energy is determined by the finite difference form of (4.32). The temperature increase occurring over each time increment Δt is summed over the duration of the run.

The handling of the viscous terms at the upper and lower boundaries of the model introduces some difficulties. Since the velocities above and below the thickness of concern are undefined, the values of the viscous terms are also undefined at the boundaries. In the initial effort the viscous effects were assumed negligible at the boundaries. However, the computed tidal forcing function for such conditions showed significant departures from their values immediately above the lower boundary and immediately below the upper, an obviously artificial state. This may have been expected since by this assumption a real boundary was assumed, i.e., a barrier to vertical transport of momentum. There is no evidence that any such real boundaries exist in these regions, instead the boundaries established were done so merely for the convenience of the problem. To overcome this shortcoming, an alternate approach to the boundary problem was taken. Both upper and lower boundaries (85 km and 110 km) were required to behave as indicated by observation, i.e., they were unaffected by other levels in the model. This restriction permitted the determination of realistic values of tidal forcing function at the levels disturbed by the initial boundary conditions.

This model was operated for three distributions of K, the smoothed curve based on calculations by Johnson and Wilkins (1965b), one half the values in this curve, and zero. The model was permitted to operate for three hours (quarter period) in each case. Figure 14 is the vector diagram

of the accelerations acting at 86 km, 92 km and 108 km in the third hour of operation (i.e., 0300 or 1500 local time.) The viscosity term has very little effect at the lower level. However, at 108 km it is of significant magnitude. The velocity vectors in this figure are given only to indicate the direction of motion and the relative speed between levels. For the case without viscosity, the TFF will lie along the vector $-\vec{f}x$ ⮟. Vectoral subtraction of the viscosity vector from the TFF (with viscosity) vector yields the TFF (without viscosity) vector.

Figure 15 is a comparison of the calculated values of TFF for the cases with viscosity and without at $t = t_o + 3$ hours. This figure demonstrates that if viscosity is ignored when attempting to infer the phase of the pressure oscillation from the wind data, the results will be a too rapid change of phase with height of the pressure oscillation. The largest errors are introduced at the higher levels. Error in phase is 24 degrees at 108 km. The magnitude of the TFF would also be underestimated over most of the height range, particularly near the top of the model. At 108 km the acceleration required to maintain the observed wind with viscosity is 180 per cent of that which is needed without viscosity. The odd and extremely large values of TFF for the viscous case at 100 km are the result of the large value of the viscous term at that altitude due to cessation of increasing amplitude with height at that level in the model. It is unlikely that the atmosphere has such a sudden change although a similar change over an altitude range of a few km would not be unlikely.

Figure 16 displays the relative magnitudes of acceleration terms as a function of altitude for this model. The Coriolis term is always

the greatest except at 100 km where a second order discontinuity resulted from forcing $\frac{\partial|V|}{\partial z}$ to become zero. The viscous term is always the smallest.

Modifications of Basic Model

The model was modified to test the effect of diurnal variation in K. The TFF was assumed to be that calculated for K given by the smooth curve approximating K determined by Johnson and Wilkins (K standard). Three basic distributions of K were tested. These were:

1) $K_{(z,t)} \equiv K_{(z)\ \text{standard}}\ (1 + .2 \sin 2\pi t/T)$

2) $K_{(z,t)} \equiv K_{(z)\ \text{standard}}\ (1 + .2 \sin [2\pi t/T + 2\pi z/L])$

3) $K_{(z,t)} \equiv K_{85\ \text{standard}}\ \exp\ (cz[1 + .3 \sin 2\pi t/T])$

where T was 24 hours and L 25 km. These three modified models were otherwise identical to the original. They were permitted to operate for 24 hours. The u component of velocities at the termination are compared to the initial values for two of the models in Figures 17 through 20. In the case of distribution 1, termination was at 23.92 hours due to program error. The difference between the change in u for the two distributions shown is relatively small (Figures 18 and 19). The results for distribution 2 are not shown because it too demonstrates great similarity. In no case was any significant region of shear generated. Distribution 3 was permitted to operate for 7 days as a test. Again, no significant region of shear was generated.

The approximated Richardson number (Ri) was included in the output of the models as an indicator of the levels most likely to experience enhancement of turbulence. It is defined as

$$Ri \equiv \frac{g}{\theta^*} \frac{\partial \theta^*}{\partial z} \Big/ \left| \frac{\partial \Psi}{\partial z} \right|^2 ,$$

where θ^* is the potential temperature in the standard atmosphere. Turbulence growth is more likely to occur when Ri is small (less than 1). The smallest value of Ri observed in any of the models was 17 which occurred at 99 km, while values at the top and the base of the models exceeded 50. These values have little meaning, however, other than to indicate the level where turbulence would be most likely to be enhanced because standard atmosphere temperature was used rather than one dependent on time.

Temperature Rise From Viscous Dissipation of Kinetic Energy

The rate of temperature increase due to the action of viscosity was determined by a difference equation based on (4.32) except eddy rather than molecular viscosity was used. The heating rate in all the modified models was very close to that of the unmodified model (Fig. 21). This heating rate is about that estimated by Hines (1965) for tidal dissipation in this region, although he based his estimates on the decrease of tidal energy with height rather than on any given value of K.

Effect of Sudden Change in Viscosity

To demonstrate the effects sudden changes in viscosity may have on the tidal wind, a simple single-level model based on (5.57) and (5.58), was constructed which determined the resultant wind as a function of time. At initial time the wind, TFF, and Coriolis vector were assumed to have the values given at 108 km in Fig. 15. The viscosity vector however was assumed zero. This approximates the situation which would exist if

the flow at this level had suddenly become purely laminar. The initial conditions are in obvious imbalance. Figure 22 displays the resultant changes with time in both speed and phase difference between the non-viscous oscillation and normal tidal oscillation. The initial displacement from the normal tidal oscillation is to the right (decrease in period) with an increase in speed. This increase in speed is accompanied by an increase in Coriolis acceleration and a reduction of the projection of TFF on the Coriolis vector. This results in a decrease in the ratio of other accelerations along the normal to the velocity vector to the Coriolis acceleration, and a retardation of phase is apparent after 8 hours. The tidal forcing acceleration continues to cause an increase in speed until the phase is retarded to the extent that the Coriolis vector lies along the TFF vector. This occurs at about 17 hours. As the phase retardation continues the TFF opposes the wind vector and a decrease in wind speed results. There results then a periodic oscillation about equilibrium.

Because the perturbation is of significant proportions and of unusual period, it would appear as a rather loud noise in any determination of tidal characteristics by superpositioning. The question as to whether similar oscillations occur in nature cannot be answered with any certainty at this time. However, speculation may be made as to how conditions favorable to the generation of such perturbations may occur. Little effort has been made to determine the variation of K in time. Richardson's criterion does indicate that K must vary significantly with changes in the vertical gradient of potential temperature. As noted earlier, in the region of interest there is a general downward flux of

heat brought about by eddy diffusivity. If for some reason this flux through a particular layer is slowed, there will be an increase in temperature immediately above due to continued downward flux in the layer above and a decrease in temperature at the bottom of the layer due to downward flux there. This results in an increase in the temperature in the upper part of the layer causing further reduction in K, a positive feedback. Thus, significant suppression of K can be visualized in relatively thin layers. If the above does occur, the effect will be somewhat less than depected in Figure 22, since molecular viscosity would remain a factor, albeit small. There would also likely be a change in the TFF because of pressure gradient change due to mass convergence. The change in TFF could be very small if the layer of increased stability was thin and restricted in horizontal extent. The generation of a single stable layer could bring about the similar development above and below. The heat buildup immediately above the initial layer will result in decreased stability there and enhanced mixing. At the top of the region of enhanced mixing another layer of increased stability would appear.

The single level model discussed above does not adequately depict what would occur in the atmosphere if K suddenly became zero, at a single level. Under such conditions, the changes in phase and amplitude at that level would bring about an increase in wind shear above and below which would likely increase K. The single level model does however, demonstrate that rapid fluctuation in K would significantly affect the tidal wind distribution.

The discussion of the effects of rapid termination of K does not necessarily apply to seasonal variation of change of phase with height.

The seasonal change in mean K at a given level should be a great deal slower. The phase shift in the first hour in the instantaneous suppression of the viscosity vector resulted in an advance of phase at a rate of 4 degrees per hour the first hour, whereas the observed seasonal change is of the order of 10 degrees per month.

In previous discussion it was tentatively assumed that K is greater in summer than in winter, throughout the region of interest, on the basis that the summer mesopause was colder than that of winter, in spite of increased heat input. This annual variation is very likely the case in the lower portion of the region of interest, but it is uncertain how high this enhancement extends. Figure 1 shows an increase of $\partial T/\partial z$ or $\partial \theta/\partial z$ in summer, over the winter value, above about 90 km. Figure 2 indicates that summer wind shear is somewhat greater than that of winter between 100 and 110 km. Larger values of Richardson number infer more rapid suppression of turbulence so it would appear that at the top of the model the winter value of K may exceed that for summer. Such a seasonal change would contribute to an explanation of the seasonal change in temperature at the mesopause. If such a reversal with height in the seasonal variation of K occurs, the height of the corssover point would certainly affect the degree of phase shift caused by viscosity.

CHAPTER VI

CONCLUSIONS

The increase with height of the coefficient of eddy viscosity requires that the viscous term be included in the equation of motion for applications in the vicinity of the mesopause. From 85 to 110 km, eddy viscosity has an increasing effect on semidiurnal tidal winds. This effect may be ignored at 85 km, but becomes important at 100 km and above. Viscosity acts to cause the change of phase with height of the tidal winds to be greater than that of pressure. The error in computing the phase of the semidiurnal pressure wave from wind data, without considering the effects of viscosity, may be as great as 24 degrees at 108 km; the amplitude of the pressure wave may be underestimated by 40% at that level.

Wave forms may be generated by periodic perturbing forces in a viscous medium. Near the mesopause such a force with a period of 12 hours results in a vertical wavelength of 8 km or less. However, the change of phase and amplitude with height of the semidiurnal tide is too small for this effect to be responsible for the large perturbations in the wind in this region.

The temperature rise due to viscous dissipation of the kinetic energy of the semidiurnal tide ranges from about .05°K per day at 85 km to 32°K per day at 110 km. These values are in general agreement with

the rates deduced by Hines by considering the decrease of tidal energy with height.

The possibility should not be overlooked that seasonal changes in eddy viscosity as a function of height are responsible for the observed seasonal phase shift and amplitude change of the semidiurnal tidal wind, although any attempt to credit viscosity with this effect is purely speculative until more is known of the variation of K in time.

If short term (order of a day) large fluctuations in K occur at isolated levels, significant perturbation of phase and amplitude of the tidal wind would occur. This effect may be a contributor to the large irregular wind variations observed near the mesosphere.

BIBLIOGRAPHY

Appleman, H. S., 1963: The climatological wind and wind variability between 150,000 and 200,000 feet, Technical Report No. 166, Air Weather Service, United States Air Force.

Chapman, S., 1924: The semidiurnal oscillation of the atmosphere, Quart. J. Roy. Met. Soc., 50, 165.

Colegrove, F. D., W. B. Hanson, and F. S. Johnson, 1965: Eddy diffusion and oxygen transport in the lower thermosphere, J. Geophys. Res., 70, 4931-4941.

Craig, R. A., 1965: The Upper Atmosphere, Academic Press, New York, 346 pp.

Friedman, J. P., 1966: Propagation of internal gravity waves in a thermally stratified atmosphere, J. Geophys. Res., 71, 1033-1054.

Georges, T. M., 1967: Evidence for the influence of atmospheric waves on ionospheric motions, J. Geophys. Res., 72, 422-425.

Greenhow, J. S., 1954: Systematic wind measurements at altitudes of 80-100 km using radio techniques from meteor trails, Philosophical Mag., 7-45, 471-490.

Greenhow, J. S., and J. E. Hall, 1960: Diurnal variations in density and scale height in the upper atmosphere, J. Atm. and Terr. Phys., 18, 203-214.

Greenhow, J. S., and E. L. Neufeld, 1955: Diurnal and seasonal wind variations in the upper atmosphere, Phil. Mag., 7-46, 549-562.

_____, 1956: The height variation of upper atmospheric winds, Phil. Mag., preprint for December issue.

_____, 1961: Winds in the upper atmosphere, Quart. J. Roy. Met. Soc., 87, 472-489.

Gringorten, I. I., R. W. Lenhard, H. A. Salmela, and N. Sissenwine, 1965: Handbook of Geophysics and Space Environment, Air Force Cambridge Research Laboratories, Cambridge, Mass.

Haltiner, G. J., and F. L. Martin, 1957: Dynamical and Physical Meteorology, New York, McGraw-Hill Book Co., 470 pp.

Hines, C. O., 1960: Internal gravity waves at ionospheric heights, Can. Jour. of Phys., 38, 1441-1481.

_____, 1963: The upper atmosphere in motion, Quart. J. Roy. Meteo. Soc., 89, 1-42.

_____, 1965: Dynamic heating of the upper atmosphere, J. Geophys. Res., 70, 177-183.

_____, 1966: Diurnal tides in the upper atmosphere, J. Geophys. Res., 71, 1453-1459.

Johnson, F. S., and E. M. Wilkins, 1965a: Thermal upper limit on eddy diffusion in the mesosphere and lower thermosphere. J. Geophys. Res., 70, 1281-1284.

_____, 1965b: Correction to "Thermal upper limit on eddy diffusion in the mesosphere and lower thermosphere", J. Geophys. Res., 70, 4063.

Justus, C. G., 1967: The eddy diffusivities, energy balance parameters, and heating rate of upper atmospheric turbulence, J. Geophys. Res., 72, 1035-1039.

Kamke, E., 1948, Differentialgleichungen, New York, Chelsea Pub. Co., 659 pp.

Kochanski, A., 1964: Atmospheric motions from sodium cloud drifts, J. Geophys. Res., 69, 3651-3662.

Lamb, H. 1932: Hydrodynamics, Dover Publications, N. Y., 738 pp.

Manring, E., J. Bedinger, H. Knaflich, and D. Layzer, 1964: An experimentally determined model for the periodic character of winds from 85 to 135 km, NASA Contractor Report, NASA CR-36, National Aeronautics and Space Administration, Washington, D.C.

Murphy, C. H., G. V. Bull, and H. D. Edwards, 1966: Ionospheric winds measured by gun-launched projectiles, J. Geophys. Res., 71, 4535-4544.

Pekeris, C. L., 1937: Atmospheric oscillations, Proc. Roy. Soc. A., 158, 650.

Richtmyer, R. D., 1957: Difference Methods for Initial Value Problems, New York, Interscience Publishers, Inc., 238 pp.

Roper, R. G., 1966: The semidiurnal tide in the lower thermosphere, J. Geophys. Res., 71, 5746-5748.

Rosenberg, N. W., and H. D. Edwards, 1964: Observations of ionospheric wind patterns through the night, J. Geophys. Res., 69, 2819-2826.

Seibert, M., 1961: Atmospheric tides, Advances in Geophysics, 7, 129-140.

Small, K. A., and S. T. Butler, 1961: The solar semidiurnal oscillation, J. Geophys. Res., 66, 3723.

Sverdrup, H. V., 1942: Oceanography for Meteorologists, Prentice Hall, Inc., New York.

Thomson, W. (Lord Kelvin), 1882: On the thermodynamic acceleration of the earth's rotation, Proc. of Roy. Soc., 11, 396.

Weekes, K., and M. V. Wilkes, 1947: Atmospheric oscillations and resonance theory, Proc. of Roy. Soc. A., 192, 80.

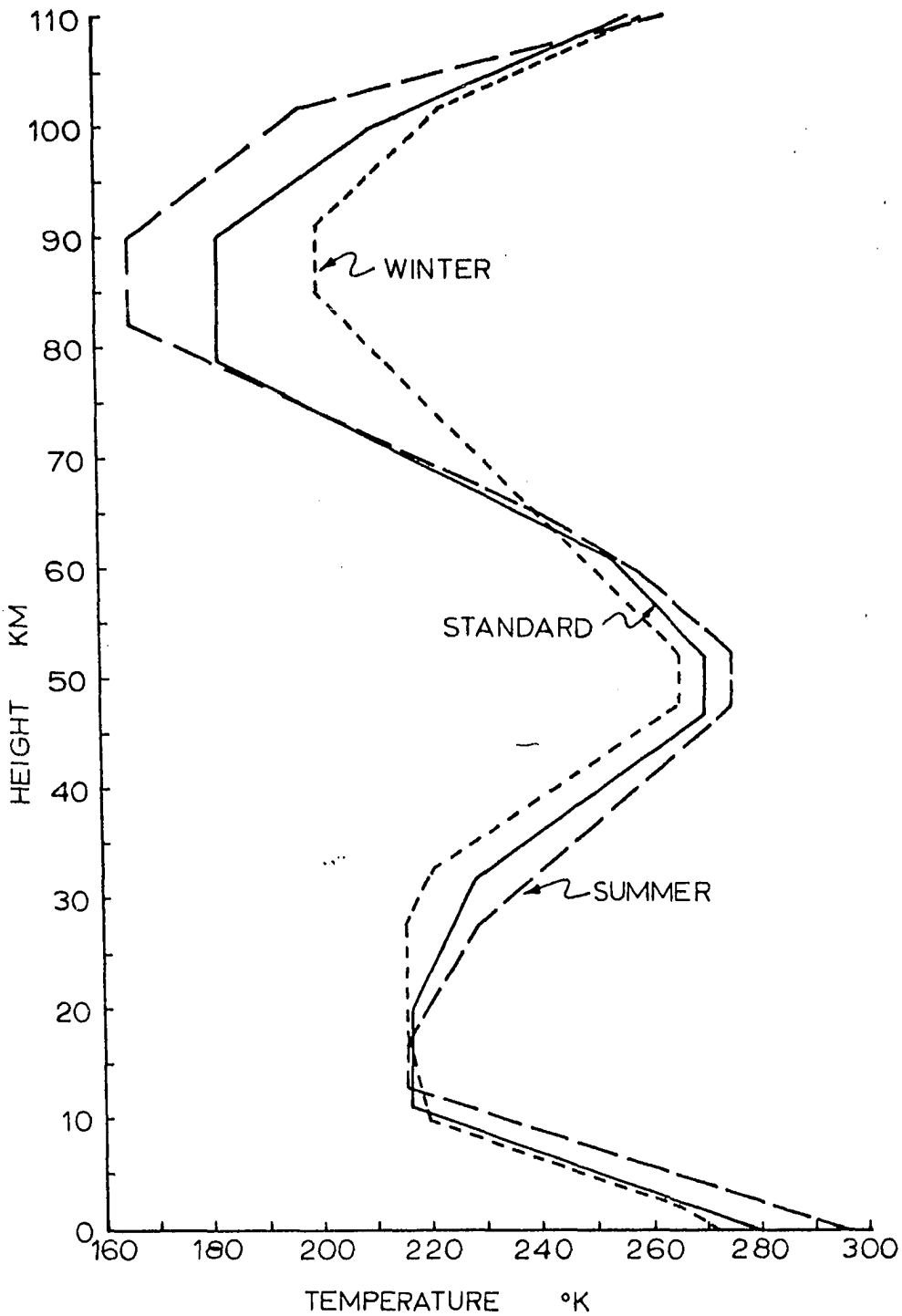

Fig. 1. Temperature distribution in height for 1962 U. S. Standard Atmosphere (COESA, 1962) and winter and summer supplemental atmospheres for 45 N (COESA, 1966)

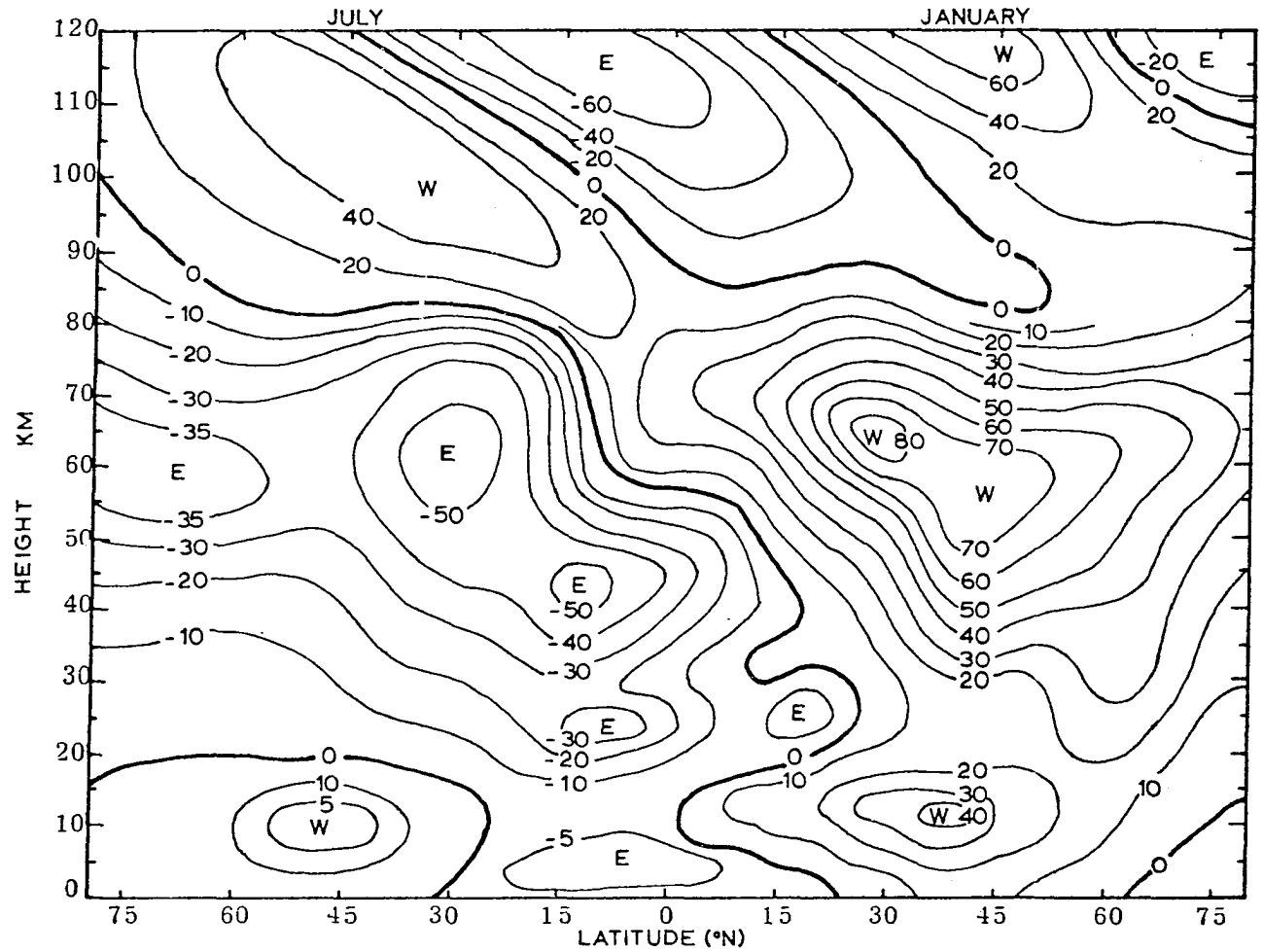

Fig. 2. Meridional cross section of the zonal wind component for January and July. (Gringorten et al.) Velocity in m sec^{-1}.

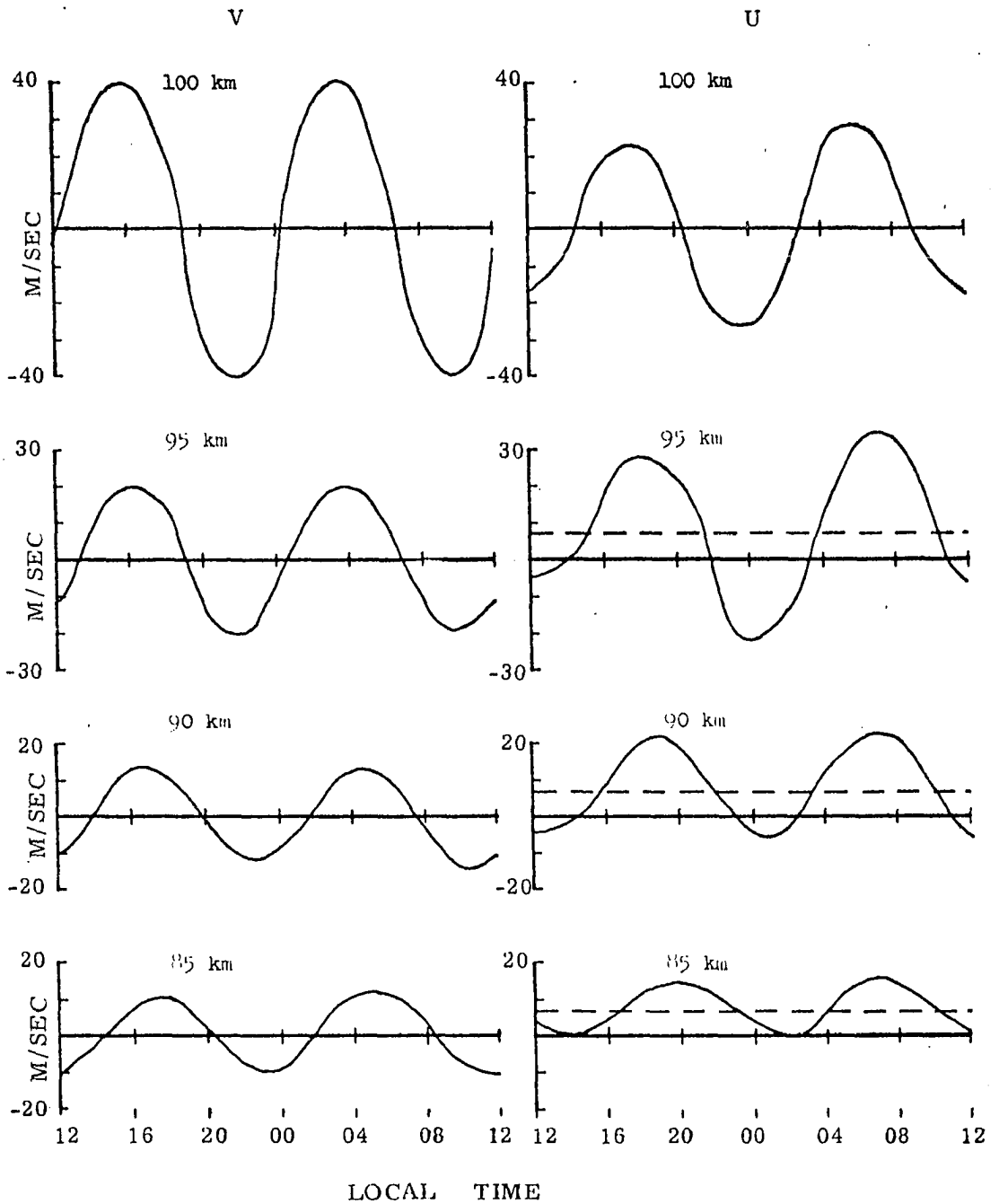

Fig. 3. Height variation of north-south, east-west wind components for Jodrell Bank for a September day (Greenhow and Neufeld, 1956)

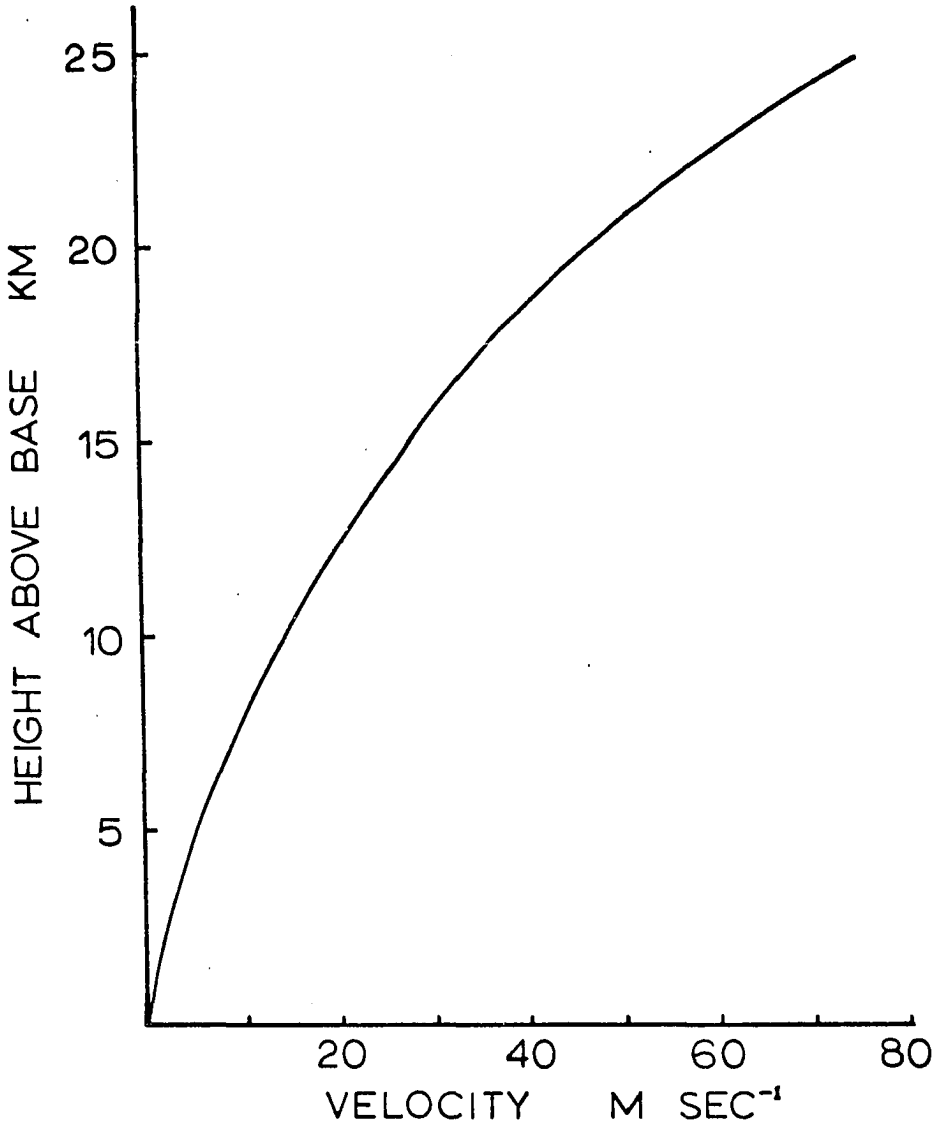

Fig. 4. Velocity profile required for $\frac{1}{\rho}\frac{\partial}{\partial z}(\rho K \frac{\partial u}{\partial z}) = 0$, for K and ρ standard and $(\partial u/\partial z)_o = .001$ sec^{-1}

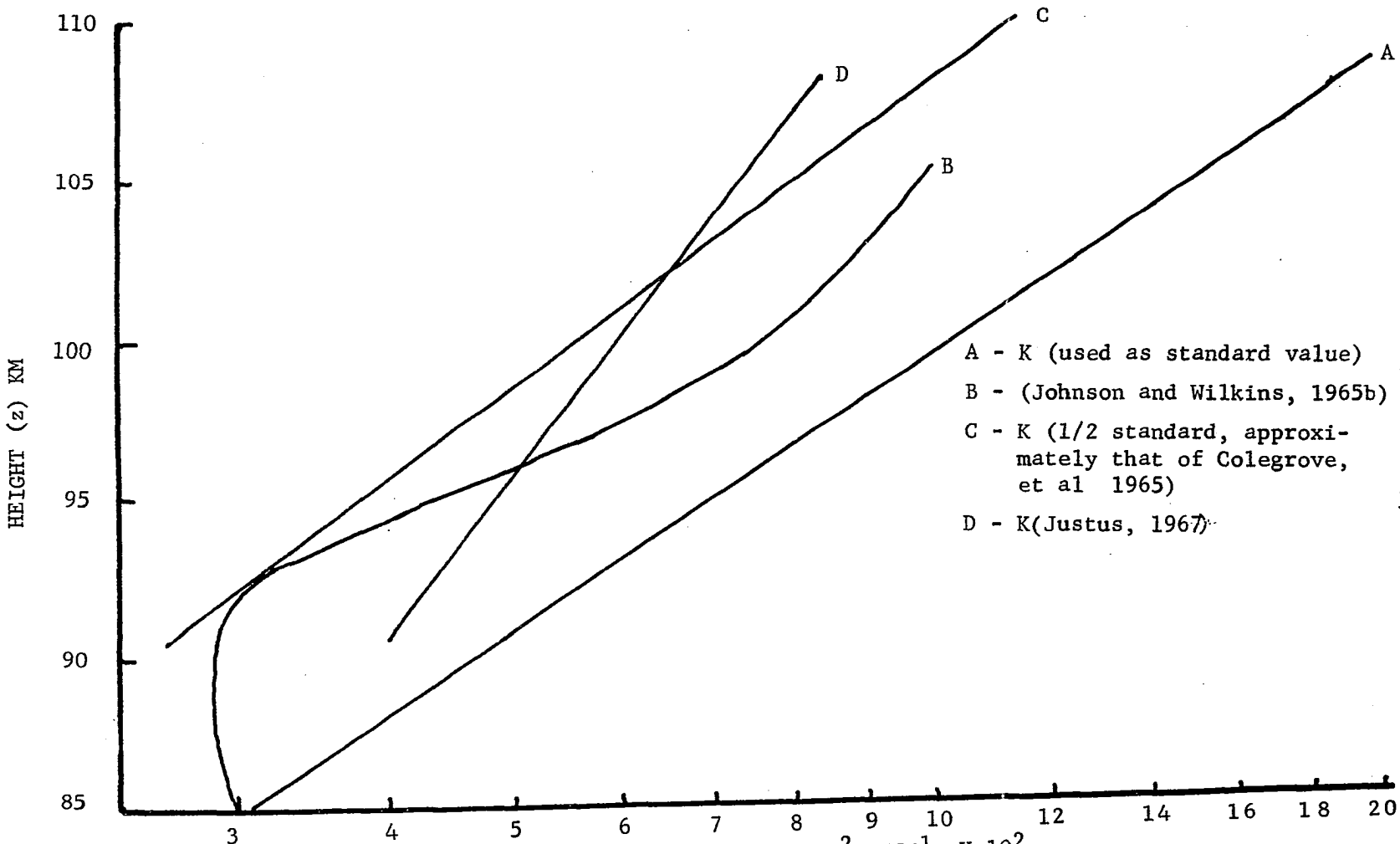

Fig. 5. Comparison of values of eddy viscosity coefficient.

FIG. 6 RELATIVE ACCELERATION DUE TO VISCOSITY ON AN INFINITE WAVE

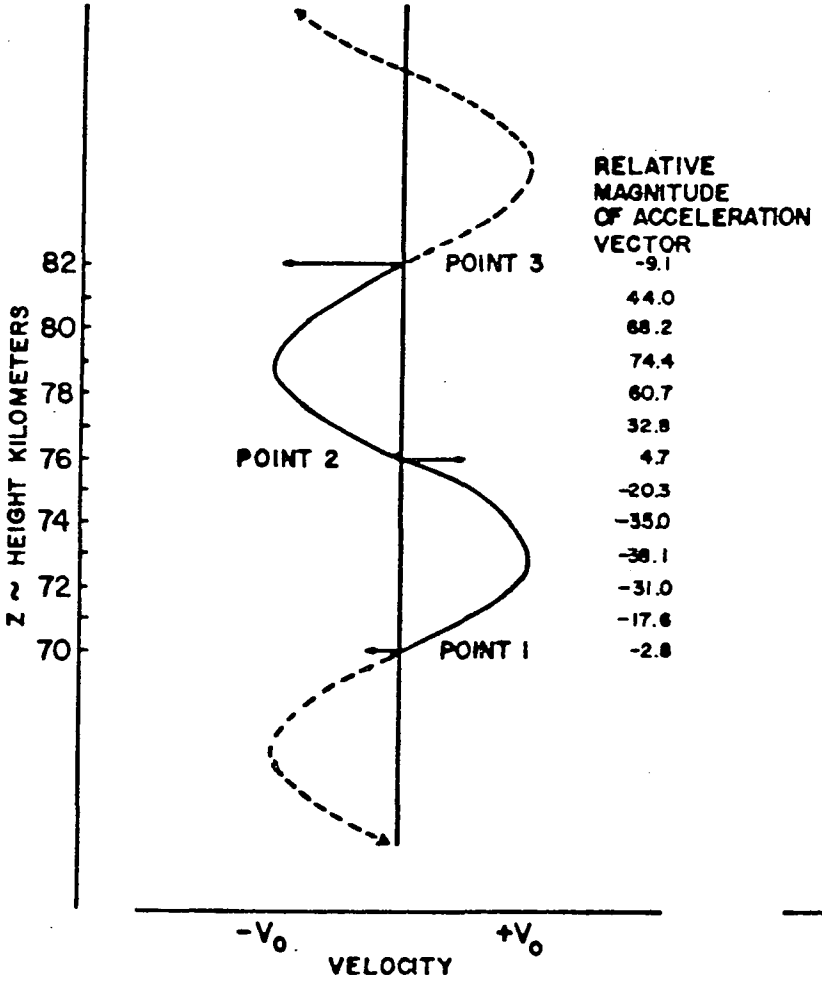

FIG. 7 RELATIVE ACCELERATION DUE TO VISCOSITY ON A FINITE PERTURBATION

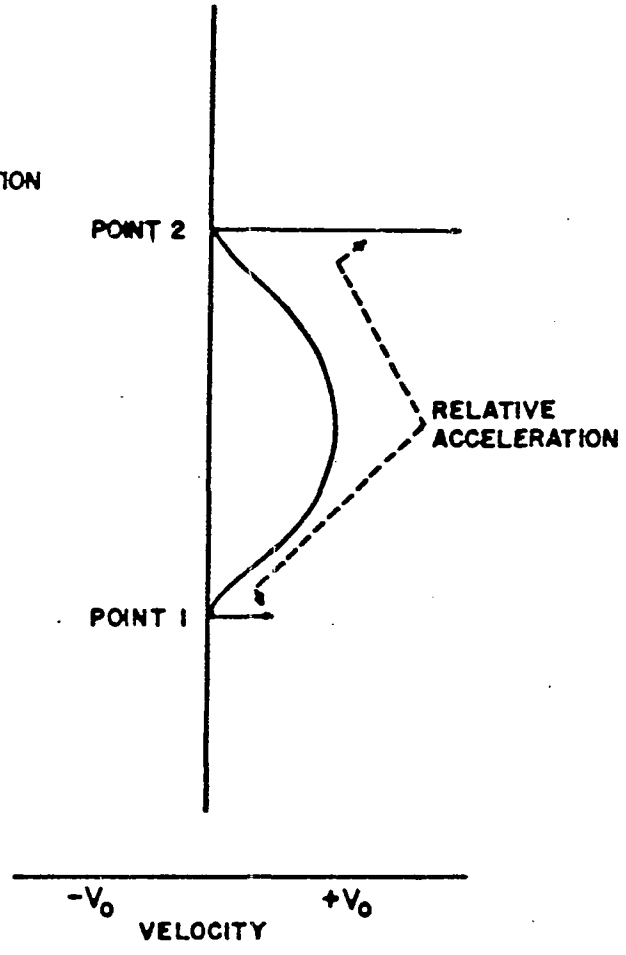

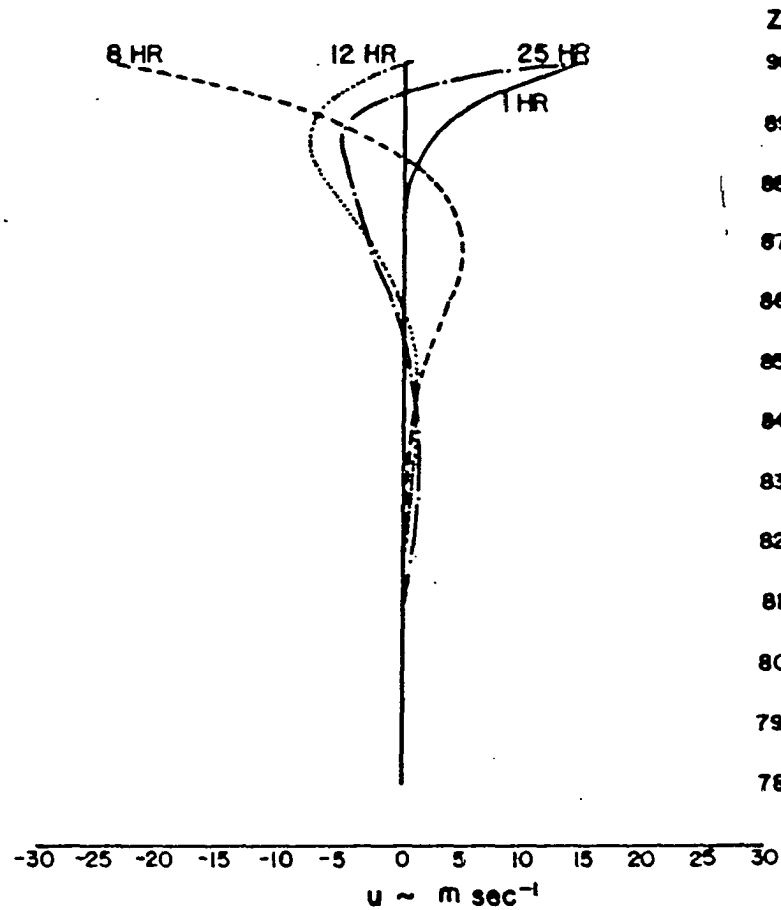

Fig. 8. Motion due to viscosity where top is forced to oscillate with period of 12 hrs. (K standard)

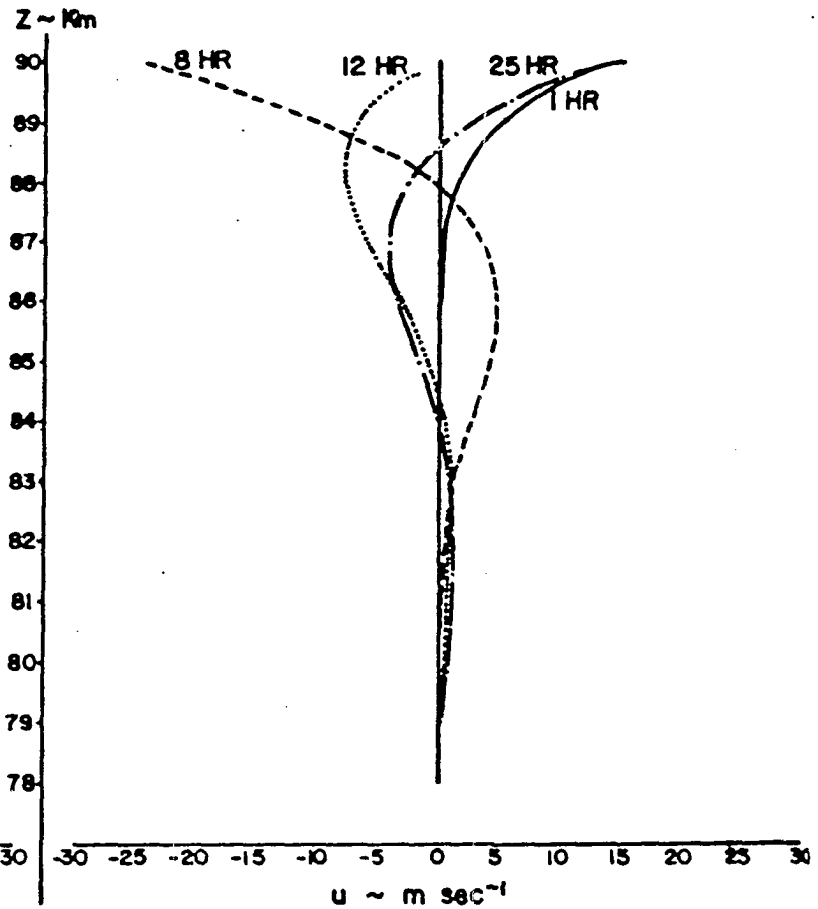

Fig. 9. Motion due to viscosity where top is forced to oscillate with period of 12 hrs. (K twice standard)

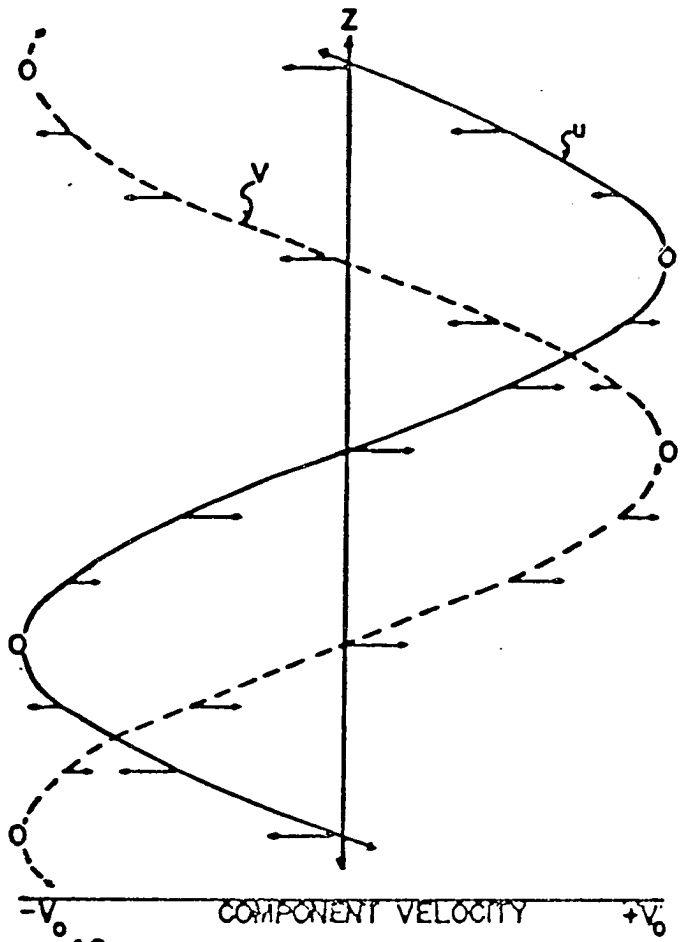

FIG. 10 RELATIVE ACCELERATION DUE TO CORIOLIS FORCE (PHASE DIFFERENCE L/4)

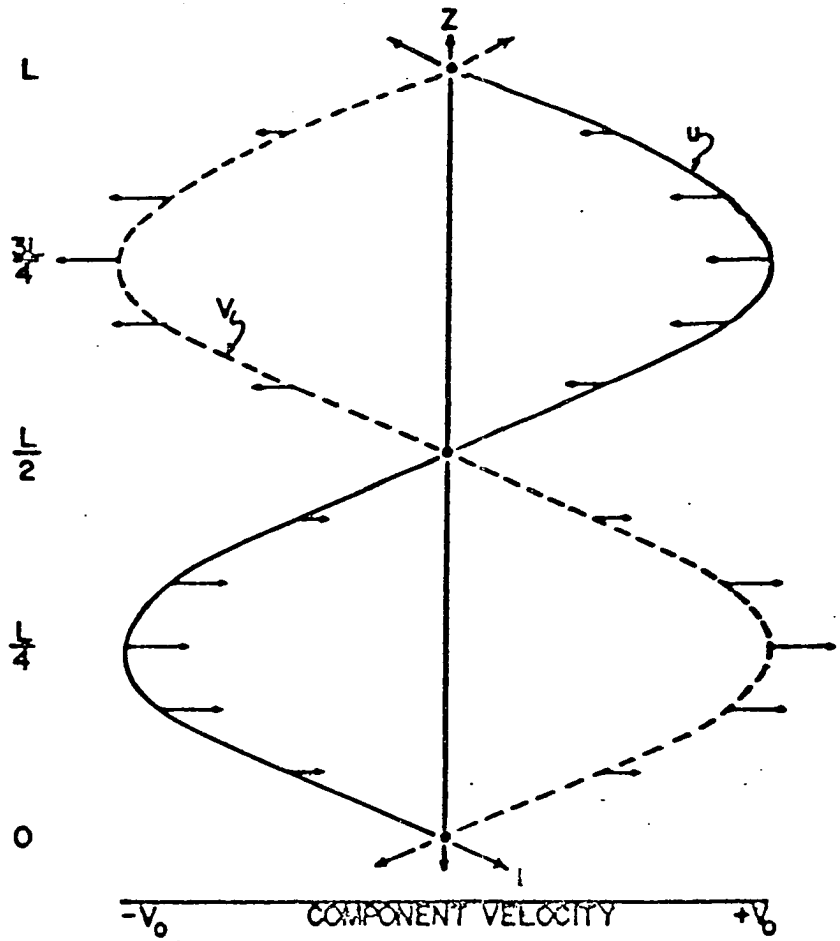

FIG. 11 RELATIVE ACCELERATION DUE TO CORIOLIS FORCE (PHASE DIFFERENCE L/2)

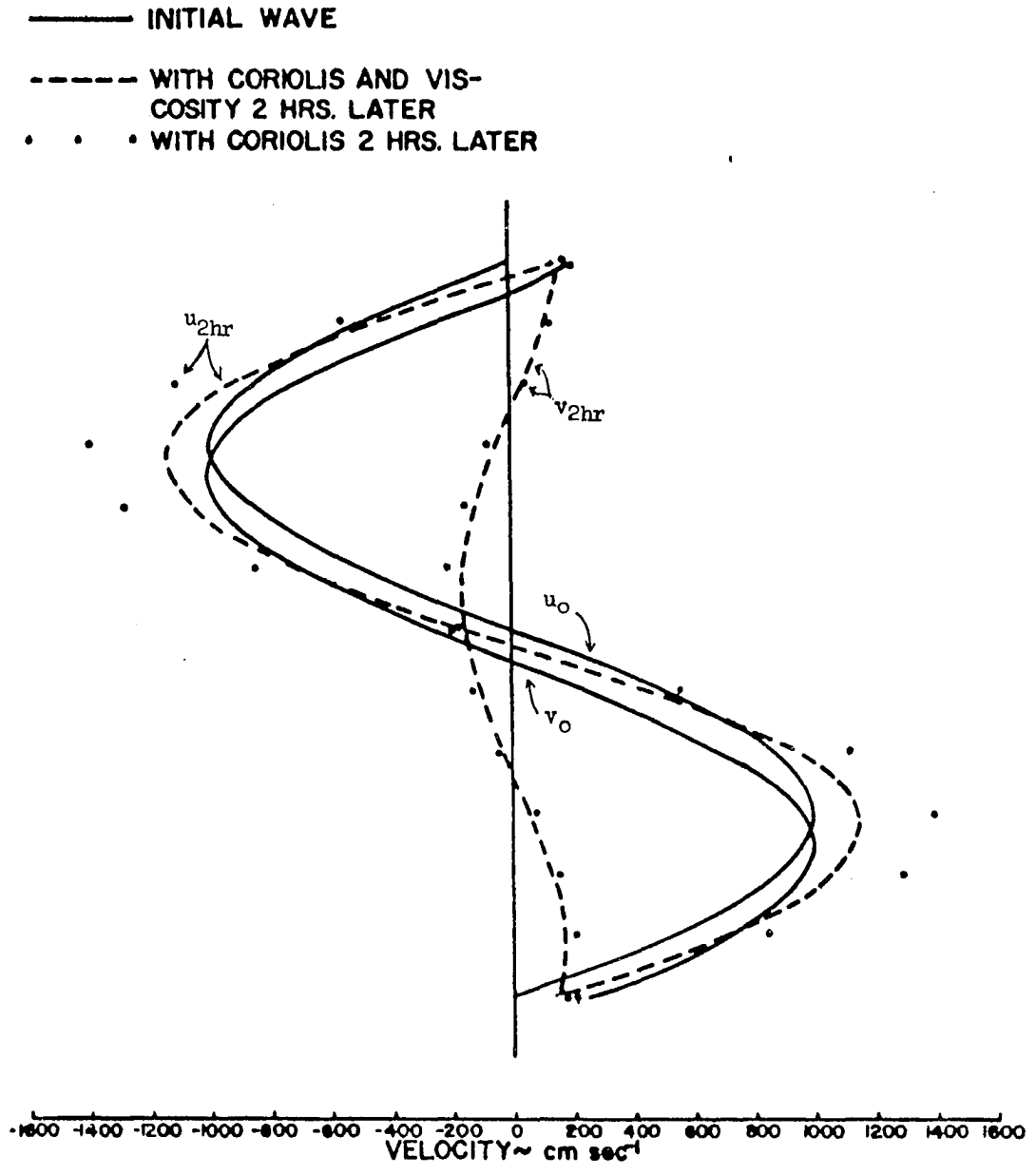

FIG. 12 EFFECT OF VISCOSITY AND CORIOLIS ON INITIAL WAVE FORM

FIG. 13 PERTURBATION INTRODUCED BY VISCOUS AND INERTIAL TERMS (TOP DRIVEN MODEL)

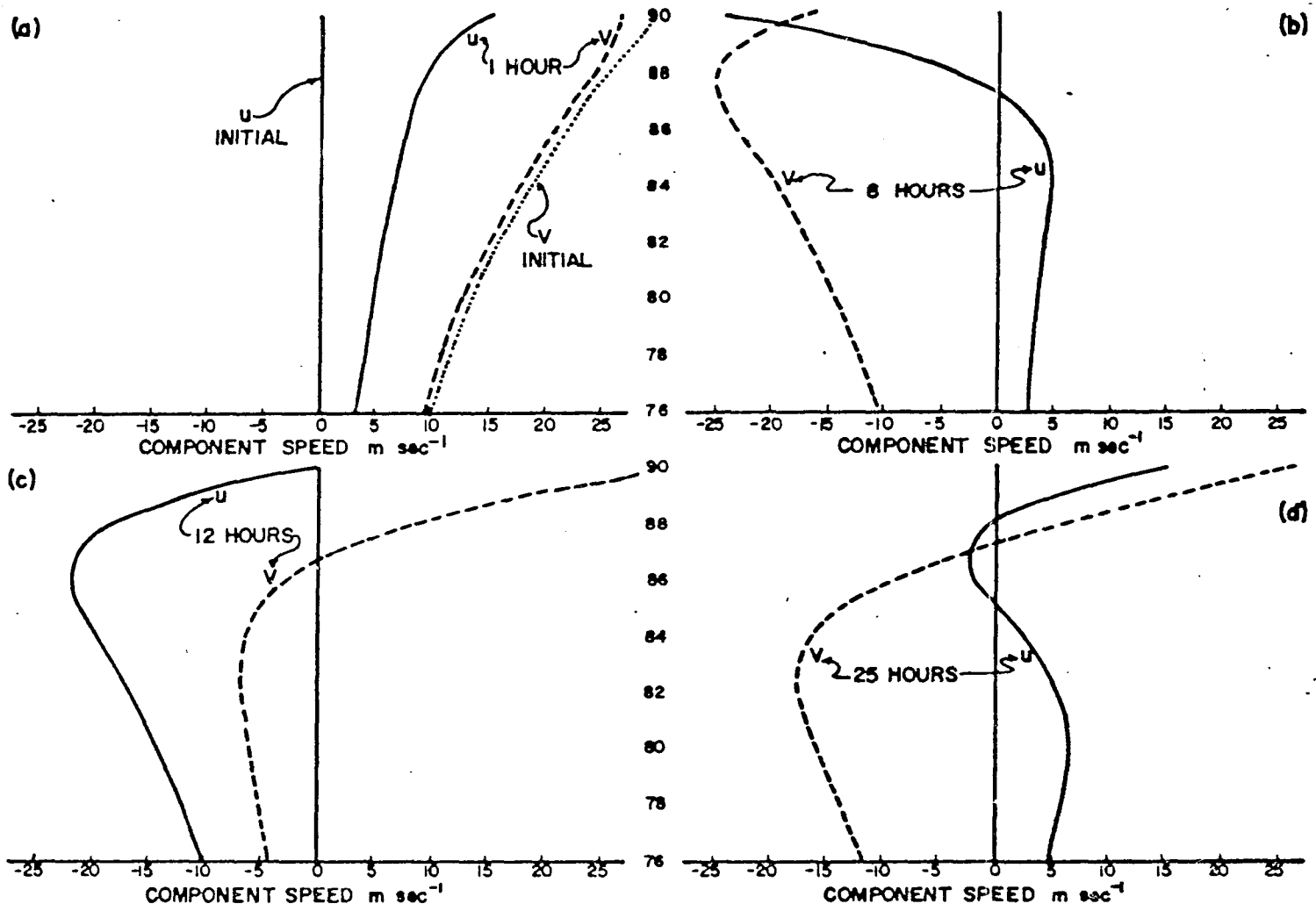

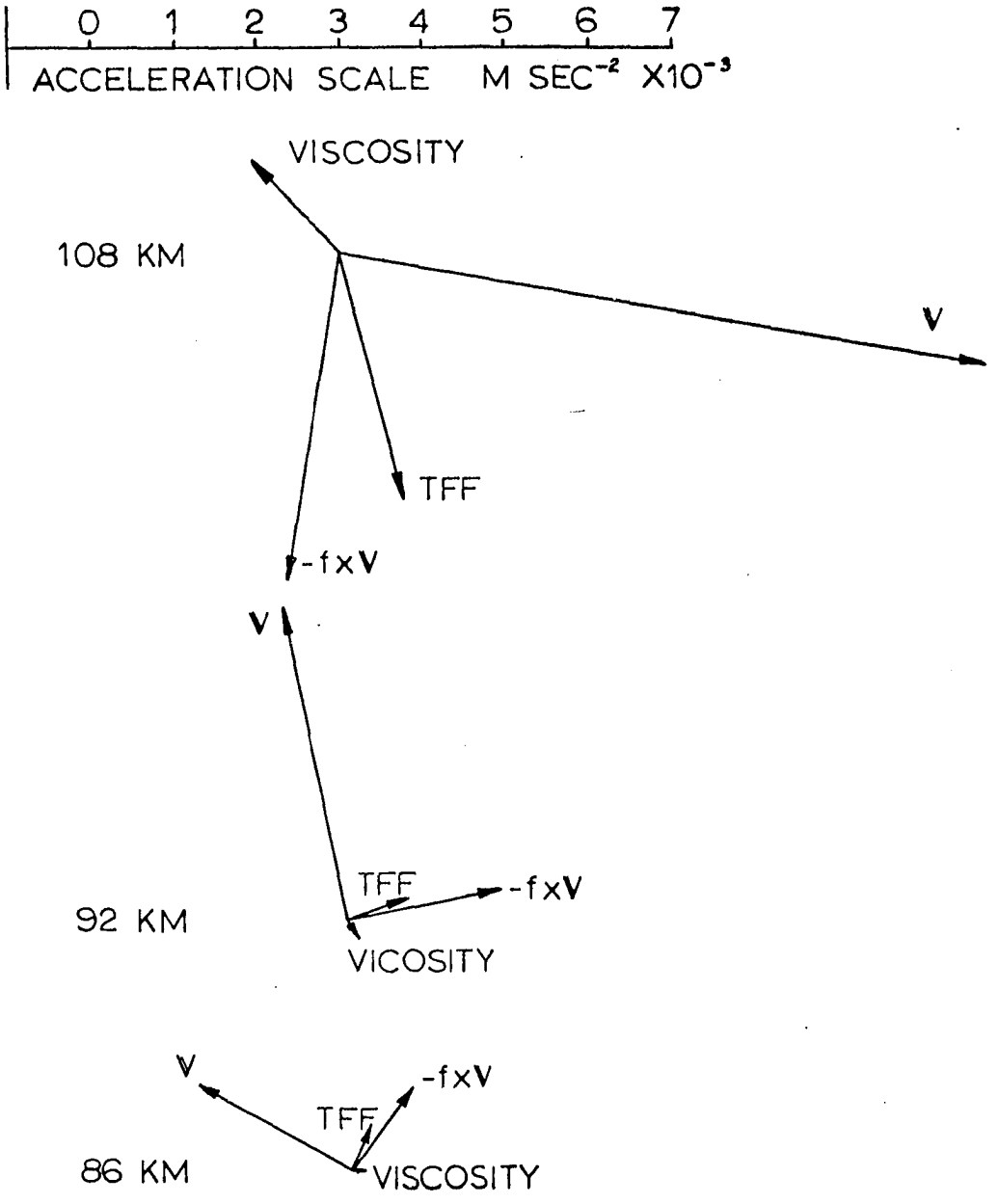

Fig. 14. Diagram of acceleration and velocity vector for 0300 or 1500 local time

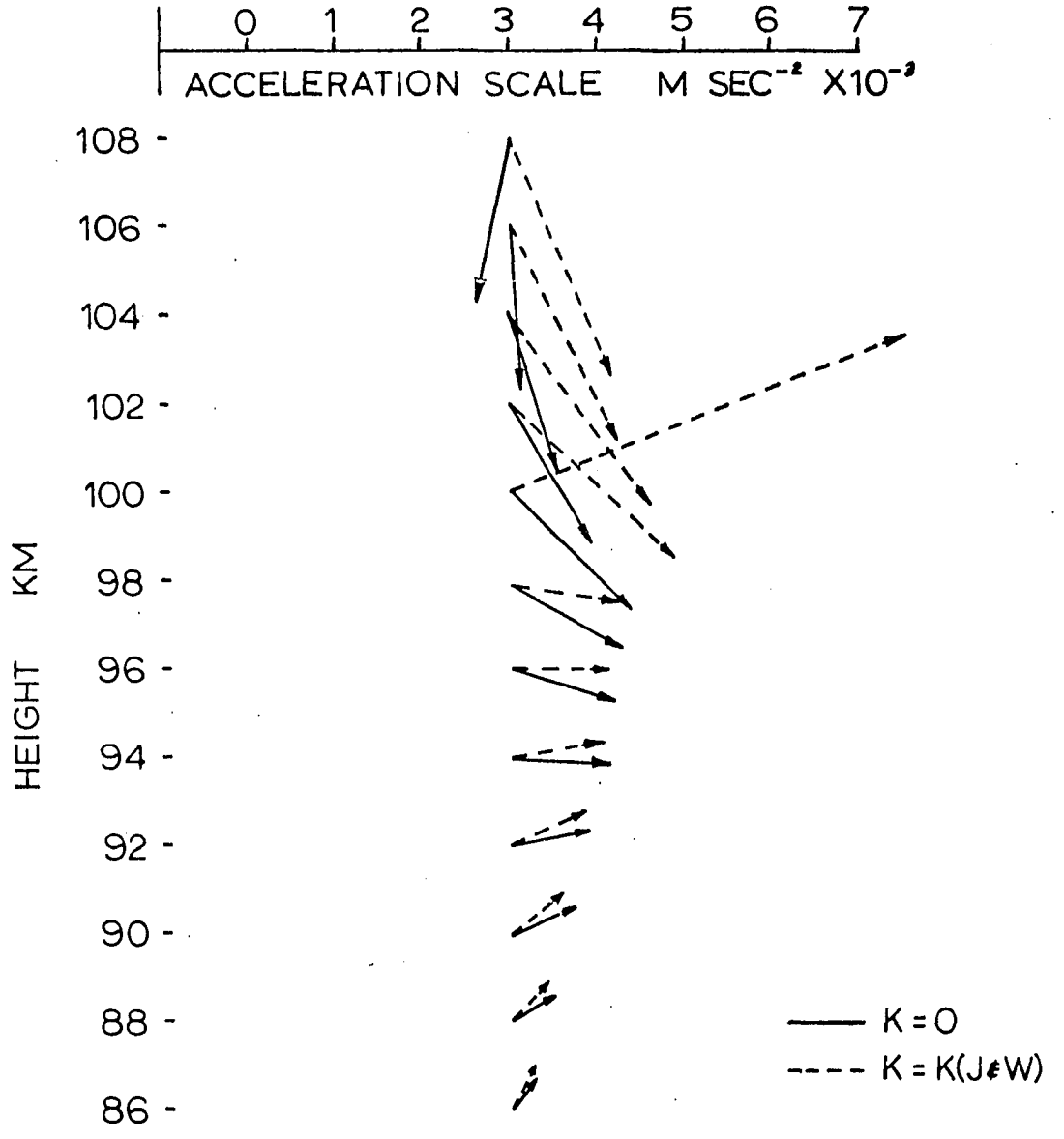

Fig. 15. Tidal forcing function required for equilibrium for K=0, K=K (Johnson and Wilkins) (local time 0300 or 1500)

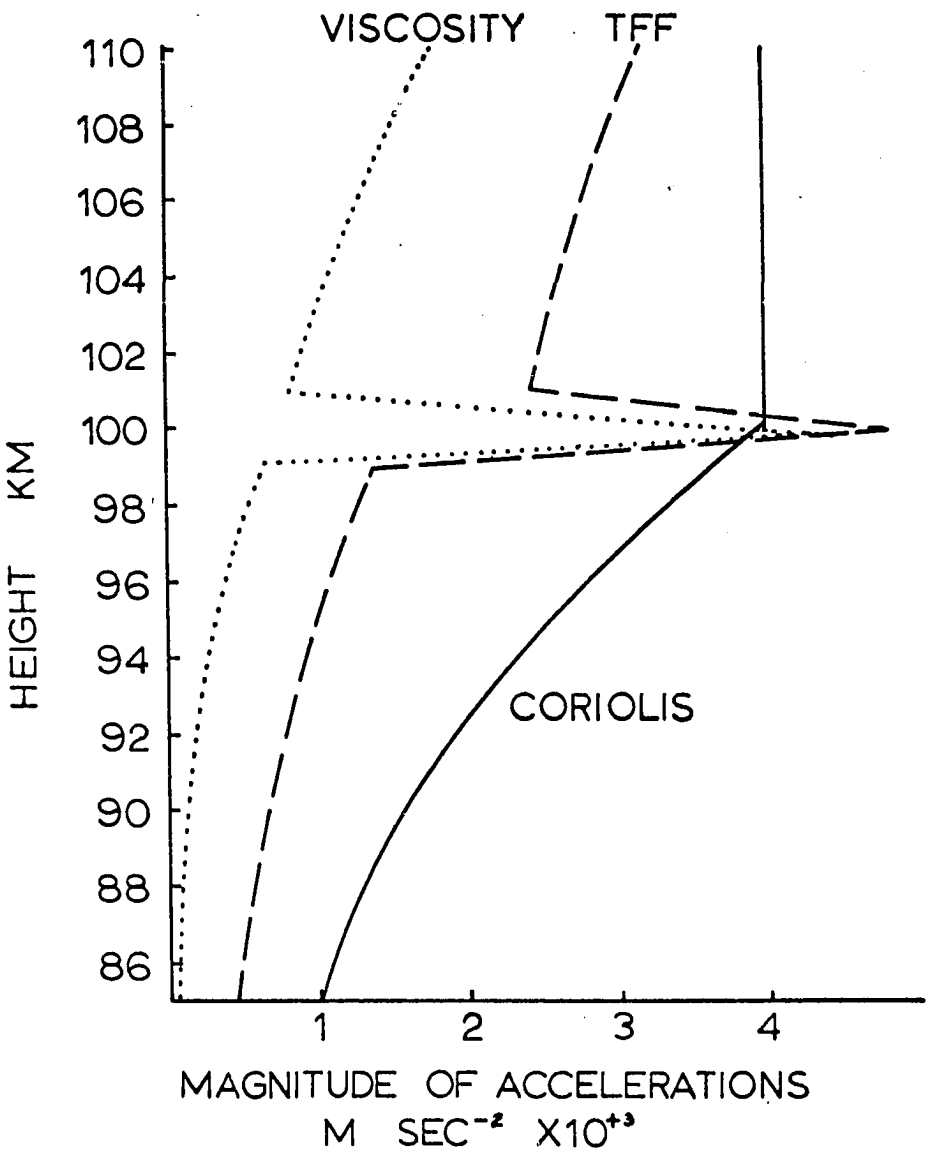

Fig. 16. Comparison of acceleration magnitudes in equilibrium

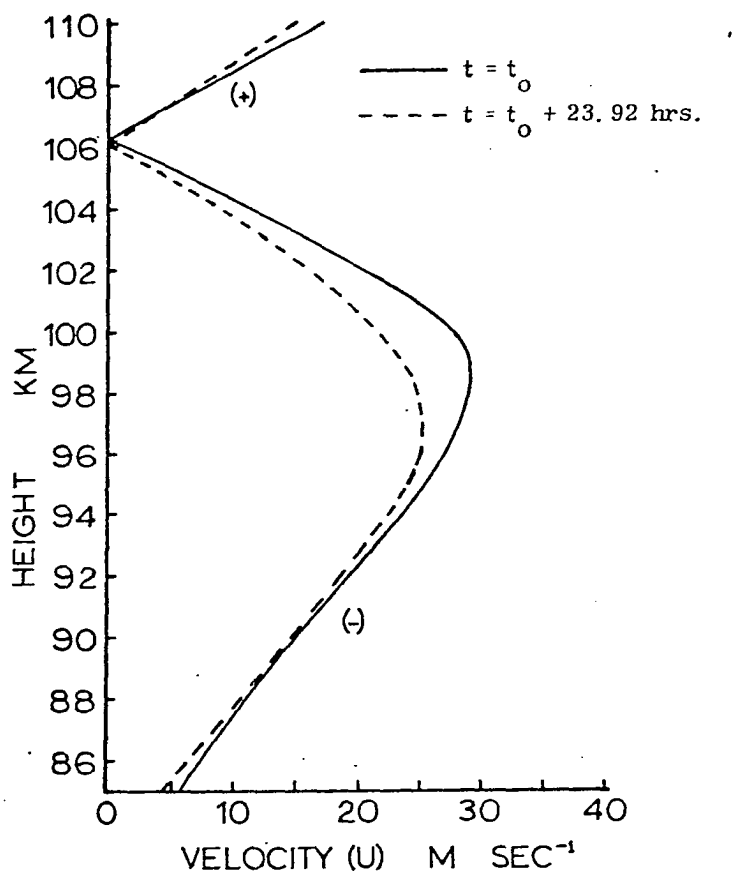

Fig. 17. Change in u component of velocity, $K = K_{standard}[1 + .2 \sin(2\pi t/T)]$ smoothed at 100 km

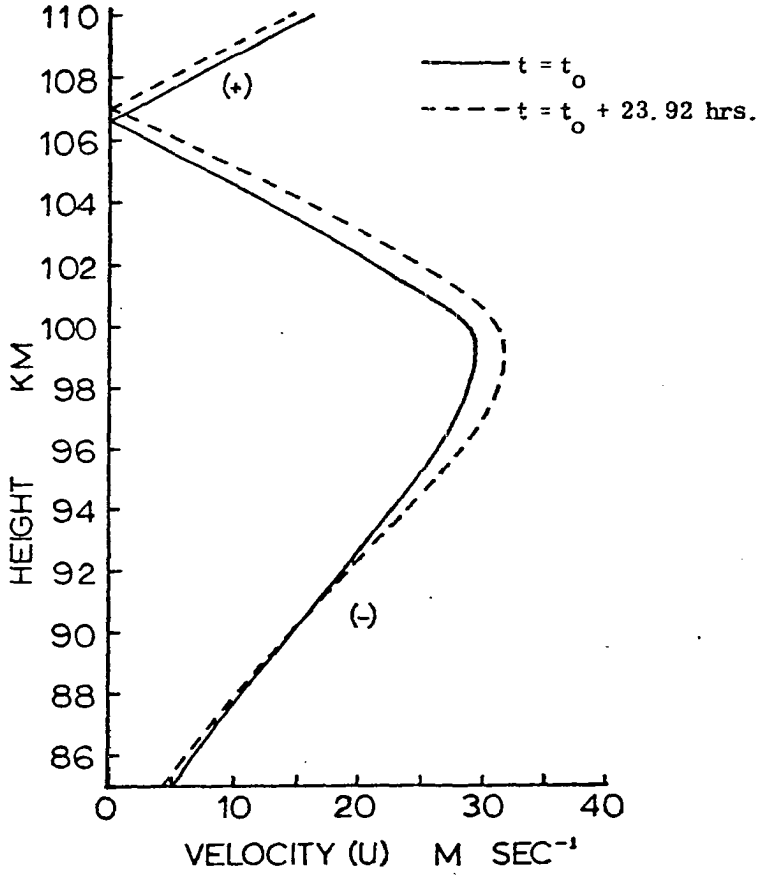

Fig. 18. Change in u component of velocity, $K = K_{standard}[1 + .2 \sin(2\pi t/T)]$ not smoothed at 100 km

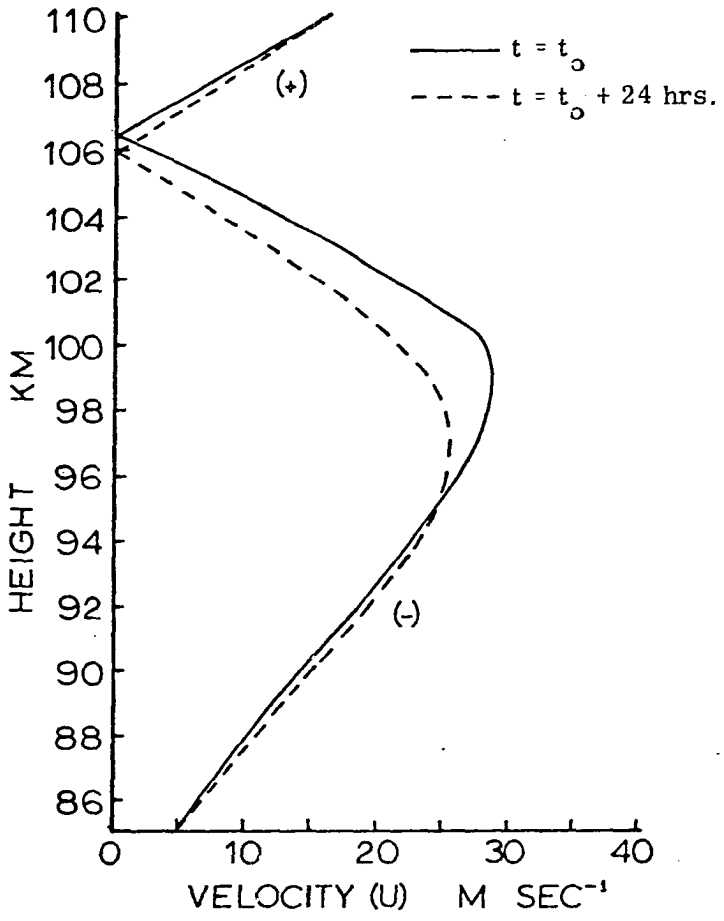

Fig. 19. Change in u component of velocity, K oscillating in height, smoothed

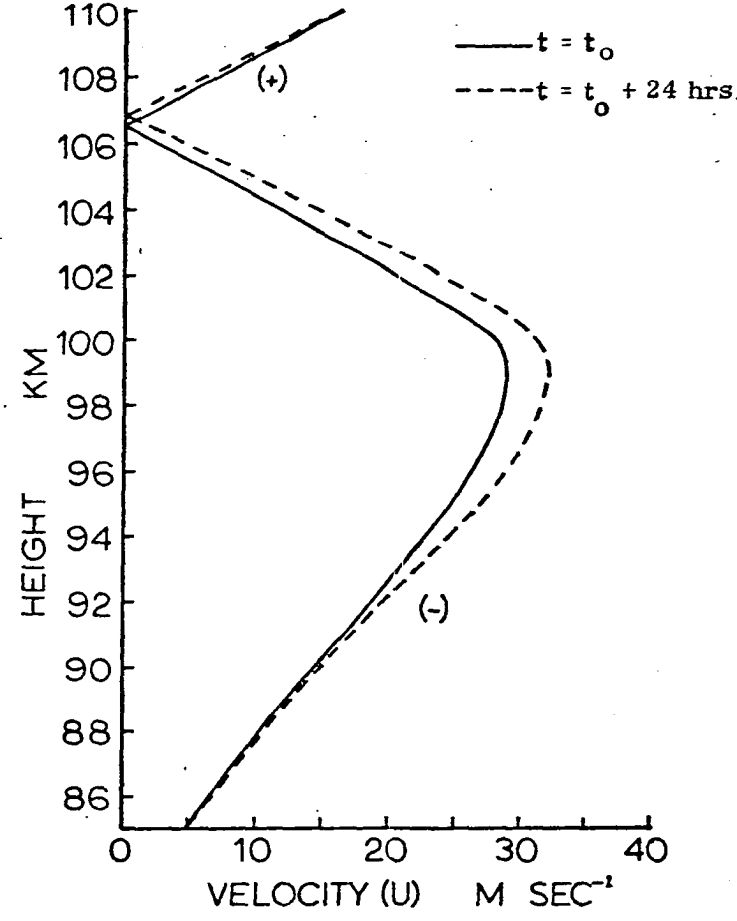

Fig. 20. Change in u component of velocity, K oscillating in height, not smoothed

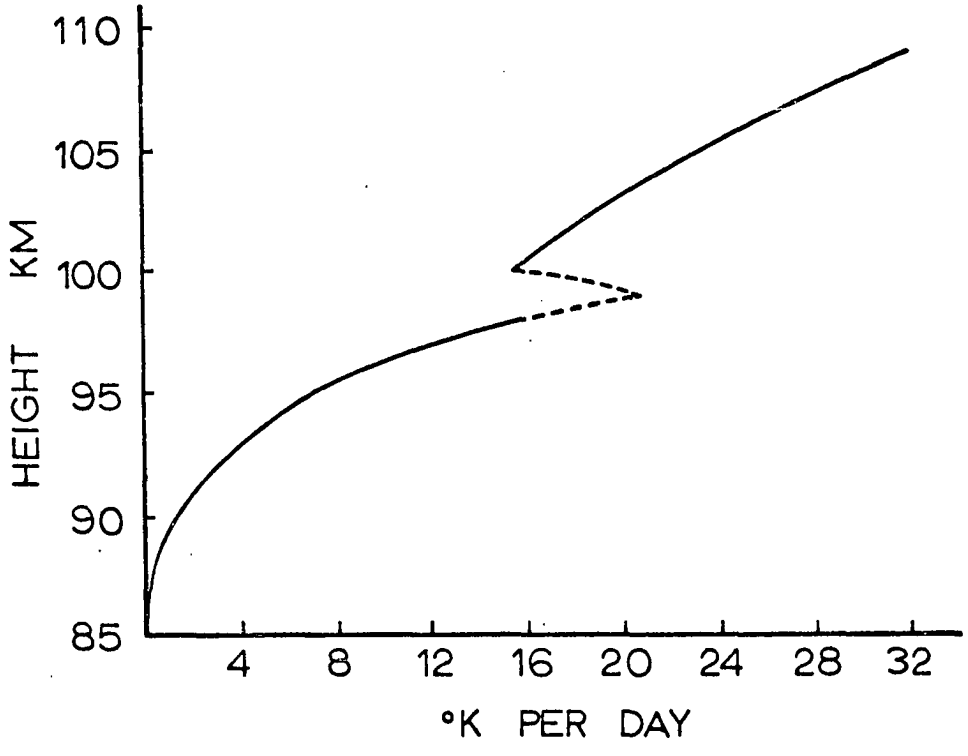

Fig. 21. Heating rate due to semidiurnal tide

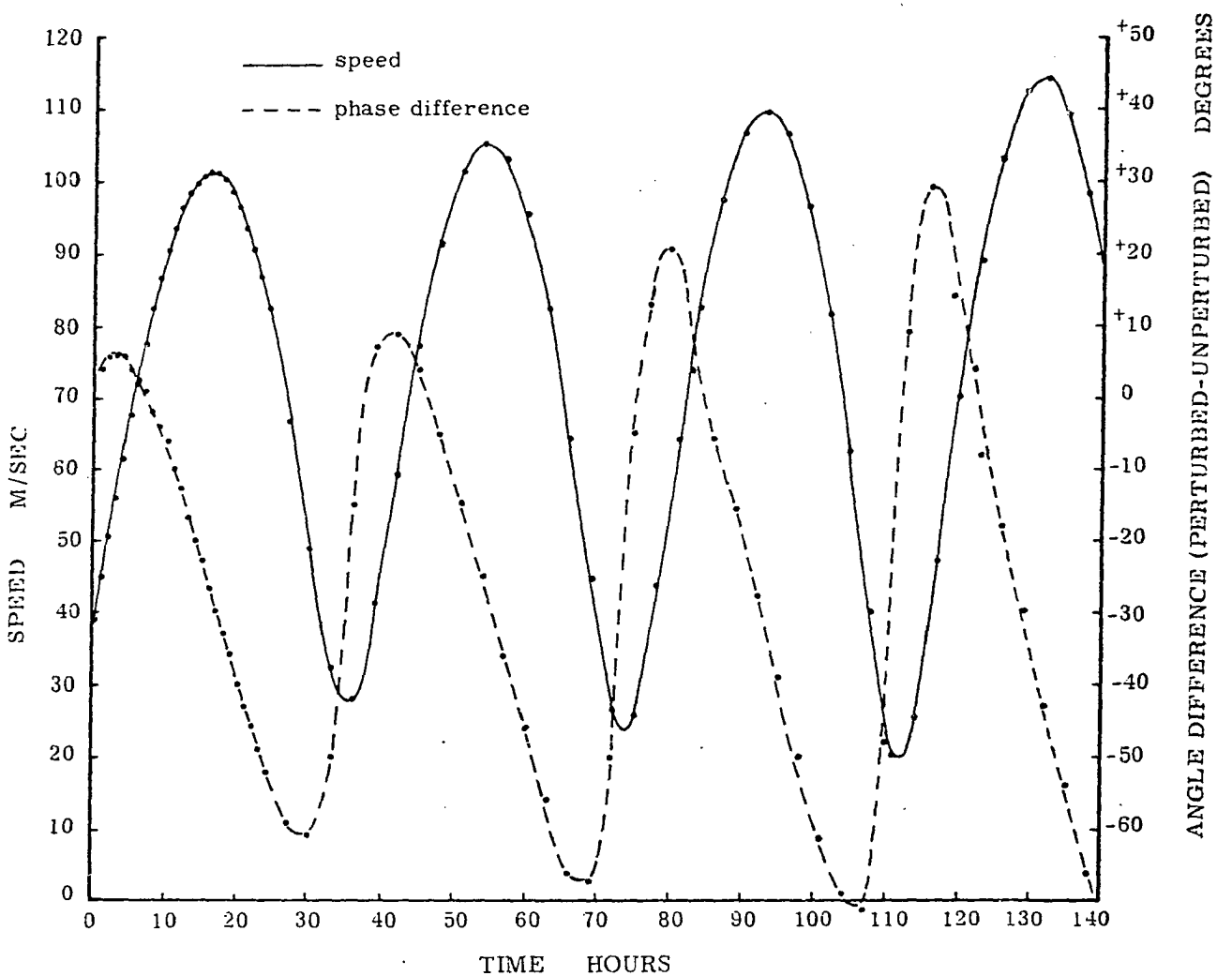

Fig. 22. Perturbation introduced by sudden decreases of K to zero at 108 km